



ELSEVIER

Contents lists available at ScienceDirect

Resources, Conservation & Recycling: X

journal homepage: www.journals.elsevier.com/resources-conservation-and-recycling-x

Advanced progress in recycling municipal and construction solid wastes for manufacturing sustainable construction materials



Zhuo Tang^a, Wengui Li^{a,*}, Vivian W.Y. Tam^b, Caihong Xue^a

^a School of Civil and Environmental Engineering, University of Technology Sydney, NSW 2007, Australia

^b School of Built Environment, Western Sydney University, NSW, 2751, Australia

ARTICLE INFO

Keywords:

Construction materials
Geopolymer composite
Municipal solid waste
Construction solid waste
Sustainability

ABSTRACT

The sharply increasing solid waste generation has raised the environmental concerns worldwide which currently have been escalated to a worrying level. Intending to eliminate the negative environmental impacts of solid waste and meanwhile promote sustainability on the energy- and resource-intensive construction and building sector, considerable efforts have been devoted to recycling solid waste for the possible use in sustainable construction material products. This paper reviews the existing studies on recycling municipal and construction solid waste for the manufacture of geopolymer composites. Special attention is paid to the predominate performance of these geopolymer composite products. The principal findings of this work reveal that municipal and construction solid waste could be successfully incorporated into geopolymer composites in the forms of precursor, aggregate, additive, reinforcement fiber, or filling material. Additionally, the results indicate that although the inclusion of such waste might depress some of the attributes of geopolymer composites, proper proportion design and suitable treatment technique could alleviate these detrimental effects and further smooth the recycling progress. Finally, a brief discussion is provided to identify the important needs in the future research and development for promoting the utilization of solid waste materials in the forthcoming sustainable geopolymer industry. In summary, this work offers guidance for the better ecological choice to municipal and construction solid waste through developing waste materials into highly environmental-friendly construction materials.

1. Introduction

Population growth, booming economy, and rapid urbanization have greatly accelerated the solid waste generation all around the world. The annual global generation of solid waste has recently approached 17 billion tons and is supposed to hit 27 billion tons by 2050 (Laurent et al., 2014). This issue is of stinging concern to the nations, municipalities, and individuals, as it can cause significant damages to human health, natural resources, and ecosystems. Therefore, the concept of adopting green chemistry and technologies for environmental sustainability has been increasingly recognized and included in recent years. Most notably, the traditional concept, in which waste is regarded as pollution, has been progressively shifting towards the new perspective that waste is treated as a resource. This undoubtedly can support

societies to become more sustainable. For instance, the energy generated in certain thermal processes of waste materials can trim the energy generation services through conventional technologies. Likewise, the reuse or recycling of certain solid waste materials, such as metal, plastic, and paper can conserve the source of the corresponding virgin materials.

Against this scenario, the research of recycling solid waste materials into the production of construction materials has been carried out extensively (De Carvalho Gomes et al., 2019). These endeavors are intended to slim down the volume of solid waste, and also trim down the mounting demand for natural resources in the construction industry. Heretofore, impressive achievements relevant to this field have been attained. For example, Huang et al. (2007) reviewed the successful utilization of solid waste materials (i.e., steel slag, waste glass, tires, and

Abbreviations: CAC, calcium aluminate cement; CFA, coal-derived fly ash; CG, coal gangue; CSW, construction solid waste; CWP, ceramic waste powder; DCP, dolomite-concrete powder; GGBFS, ground granulated blast furnace slag; MIBA, municipal solid waste incineration bottom ash; MIFA, municipal solid waste incineration fly ash; MK, metakaolin; MSW, municipal solid waste; NP, natural pozzolana; nS, nano-SiO₂; OPC, ordinary Portland cement; RT, room temperature; S/S, stabilization/solidification; SiMn, silico-manganese; TMWM, Tungsten mining waste mud; WCB, waste clay brick; WCP, waste concrete powder; WGP, waste glass powder; WPSA, waste paper sludge ash

* Corresponding author: School of Civil and Environmental Engineering, University of Technology Sydney, NSW 2007, Australia

E-mail address: wengui.li@uts.edu.au (W. Li).

<https://doi.org/10.1016/j.rcrx.2020.100036>

Available online 06 March 2020

2590-289X/ © 2020 Published by Elsevier B.V. This is an open access article under the CC BY-NC-ND license

(<http://creativecommons.org/licenses/by-nc-nd/4.0/>).

plastics, etc.) for the development of asphalt pavements. Meng et al. (2018) summarized the existing research work on recycling a range of solid waste materials in the production of concrete blocks, including crushed brick, waste glass, recycled concrete, ceramic waste, and tile waste, etc. Luhr et al. (2019b) outlined the possible use of various kinds of aquacultural and agricultural farming waste as supplementary materials in concrete.

Besides that, some attracting achievements have been made in recycling solid waste materials for the manufacture of geopolymer composites. Geopolymer, namely alkali-activated material, is usually derived from the chemical reaction between aluminosilicate precursor materials and alkaline activators, being widely regarded as an alternative to ordinary Portland cement (OPC) (Provis, 2013). The past three decades have witnessed the rapid development of geopolymer through academic pursuit because of its excellent performance in various fields. In general, geopolymer exhibits excellent mechanical properties and other inherent properties such as superior durability, immobilization of toxic contaminants, or even multifunctionality and intelligence (Ji and Pei, 2019; Provis, 2013; Tang et al., 2019b). Furthermore, geopolymer is featured with low greenhouse-gas emissions, less energy consumption, and reuse of waste materials, which is considered critical to the future sustainability of the building and construction industry (Habert et al., 2011; Hassan et al., 2019). Thus, exploiting the potential of using solid waste materials as a component in geopolymer composites will certainly contribute to a greener and more sustainable construction material. Generally, solid waste is mainly composed of the municipal, industrial, construction, and agriculture solid wastes (Hoorweg and Bhada-Tata, 2012). In literature, the utilization of solid waste such as industrial waste and agricultural waste in the manufacturing of geopolymer composites has been well documented (Part et al., 2015).

This paper, therefore, deals with the anthology and analyses of the achievements previously attained when municipal and construction solid waste was employed in geopolymer composites manufacturing. In addition, the benefits and limitations of these resulted geopolymer composites incorporating municipal and construction solid waste are evaluated. Overall, this work hopes to offer a scientific foundation for the upcoming development of geopolymer composites, which is featured with high eco-friendliness.

2. Municipal solid waste

Municipal solid waste (MSW) generally refers to domestic and commercial waste generated within the jurisdiction of a municipal authority. In most cases, MSW mainly consists of organic material, waste paper, waste glass, plastic waste, tin cans, textiles, etc. With the world hurtling toward the urban future, the growth rate of MSW has exceeded the speed of urbanization (Sun et al., 2018). It has been

reported that the global MSW per annum is expected to reach 2.2 billion by 2025, which is tripled of 0.68 billion in 2002 (Hoorweg and Bhada-Tata, 2012). Fig. 1 presents the annual MSW generation from the selected countries (Waste Atlas, 2019). Consequently, researchers have attempted to employ this waste for the preparation of geopolymer composites. Surprisingly, they have encountered exciting and impressive discoveries in this regard. Therefore, this section deals with the emerging research studies on recycling MSW into geopolymer composites, including municipal solid waste incinerator ash, waste paper, rubber waste, plastic waste, along with some others.

2.1. Municipal solid waste incineration ash

Currently, incineration is commonly used practice against the context of substantial MSW. Incineration can reduce waste volume and mass by up to 90 % and 70 %, respectively (Silva et al., 2019b). Additionally, incineration allows for producing energy from waste. While after the incineration process, two types of ashes are generated, namely municipal solid waste incineration bottom ash (MIBA) and municipal solid waste incineration fly ash (MIFA). MIBA is the residue with large particles, which is found at the bed of the incinerator, whereas MIFA corresponds to the very fine particles collected by the air pollution control system (Sarmiento et al., 2019). As different characteristics of MIBA and MIFA, their utilization in geopolymer composites is discussed below separately.

2.1.1. MIBA

MIBA accounts for about 80 % of the waste combustion residues and contains much less toxic organic substances in comparison with MIFA. Thus, there exists a great potential for the utilization of MIBA rather than sending it to a landfill. Although there have been considerable efforts to valorize this waste through using it as raw material for cement production or as filler for road construction, several significant drawbacks limit the wide applications of MIBA, especially the leach of heavy metals (Siddique, 2010a).

The chemical composition of the MIBA from the select studies is presented in Fig. 2(a), including the average value as well as the minimum and maximum values. Also, the mineralogy of MIBA is provided in Fig. 2(b). Obviously, MIBA can potentially be utilized as a geopolymer precursor, due to the presence of both amorphous fraction, and high content silica and aluminum oxide. Initially, MIBA was used as a partial replacement for the precursors during the synthesis of geopolymer composites (Lancellotti et al., 2013). Lancellotti et al. (2013) demonstrated that MIBA was suitable source material for producing metakaolin blended geopolymers, with the contents up to 70 % of the precursor. The follow-up studies then examined the feasibility of using MIBA as the only geopolymer precursor (Chen et al., 2016; Lancellotti

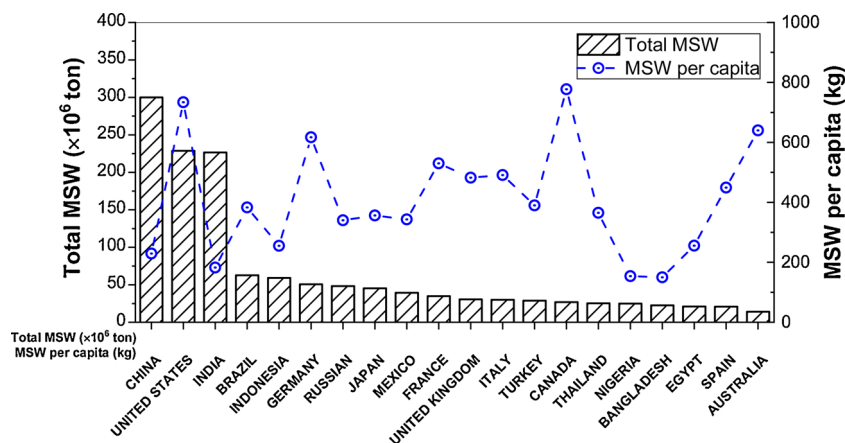


Fig. 1. Annual MSW generation from selected countries (Waste Atlas, 2019).

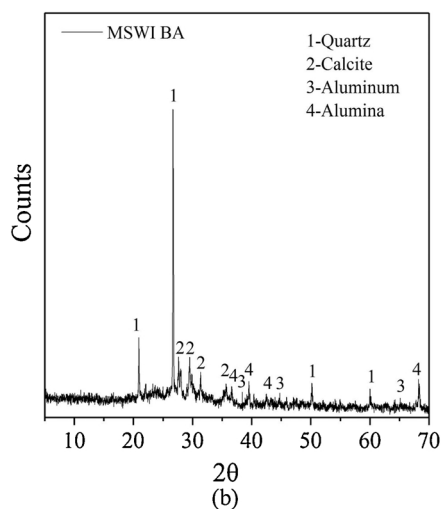
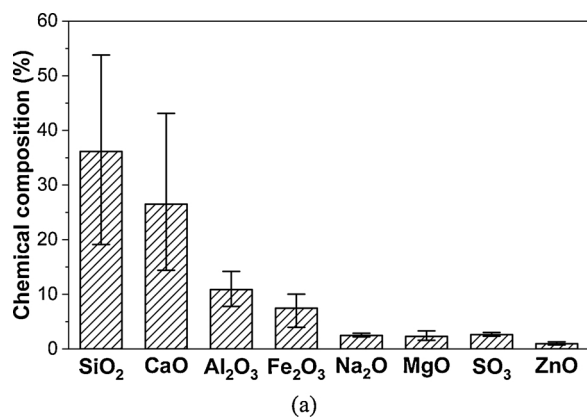
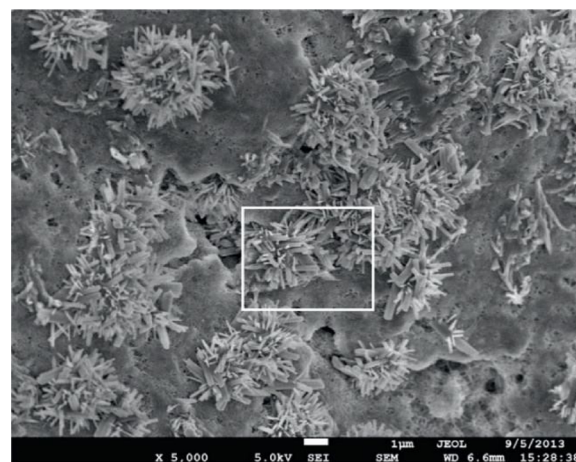


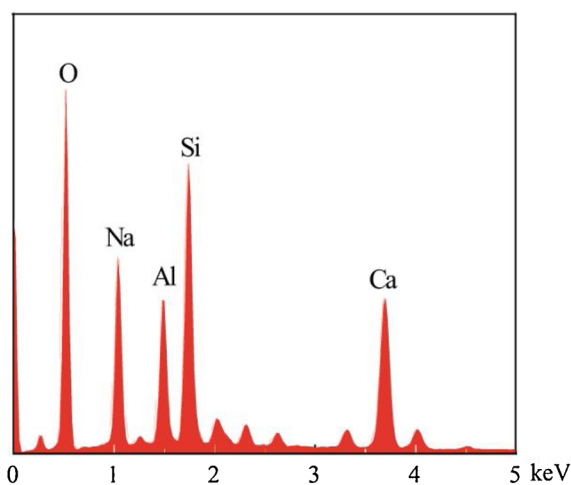
Fig. 2. Chemical composition and mineralogy of MIBA: (a) Chemical composition of MIBA from the selected studies. Data from [Chen et al. \(2016\)](#); [Gao et al. \(2017\)](#); [Huang et al. \(2018b\)](#), a; [Xuan et al. \(2019\)](#); [Zhu et al. \(2018\)](#); (b) XRD pattern of MIFA (1, CaClOH; 2, NaCl; 3, KCl; 4, SiO₂; 5, CaCO₃) ([Li et al., 2019](#)).

[et al., 2015](#); [Zhu et al., 2019a](#)). For instance, through microstructure analysis and composition characterization, [Chen et al. \(2016\)](#) have identified the successful geopolymerization of MIBA, and the formation of new crystal phase consisting of silica, aluminum, and sodium, as shown in [Fig. 3](#). Similar results have also been observed in the studies by [Lancellotti et al. \(2015\)](#) and [Zhu et al. \(2019a\)](#). Furthermore, numerous studies have investigated the heavy metal binding effect of MIBA-based geopolymer composites. It is consistently believed that geopolymerization is able to immobilize the majority of hazardous elements in MIBA effectively, and the produced geopolymer composites can be characterized as non-hazardous materials ([Chen et al., 2016](#); [Gao et al., 2017](#); [Zhu et al., 2019b](#)).

It should, however, be noted that the resulting MIBA-based geopolymer composites usually possess low mechanical performance and highly porous structure ([Lancellotti et al., 2015](#)). This is mainly attributed to that the metallic aluminum presented in MIBA can react with alkaline solution and then generate hydrogen gas ([Chen et al., 2016](#)). Consequently, MIBA has been employed as the precursor partially or fully to synthesize aerated geopolymer composites ([Chen et al., 2016](#); [Xuan et al., 2019](#)). [Chen et al. \(2016\)](#) produced the MIBA aerated geopolymer pastes with the dry density ranging from 600 kg/m³ to 1000 kg/m³. The test results also showed that the alkaline concentration, the ratio of liquid to solid, and mixing duration were the important factors in controlling the physical and mechanical properties of the produced MIBA aerated geopolymer. Likewise, in the study of [Xuan et al. \(2019\)](#), the aerated geopolymer pastes synthesized by integrating the utilization of MIBA and waste glass powder exhibited low density



(a)



(b)

Fig. 3. SEM/EDX of Na-Si-Al system crystal in MIBA geopolymer: (a) Microstructures by SEM; (b) EDX spectrum ([Chen et al., 2016](#)).

values ranging from 494 kg/m³ to 1295 kg/m³, and low thermal conductivities ranging from 0.14 W/m·K to 0.38 W/m·K. Besides, in comparison with the traditional aerated concrete, the prepared aerated geopolymer concrete had less spherical air voids and wider air-void size distribution ([Xuan et al., 2019](#)).

Additionally, researchers adopted MIBA as a gas-forming additive to aerate geopolymer composites ([Zhu et al., 2018, 2019b](#)). For instance, [Zhu et al. \(2018\)](#) compared the effects of MIBA and commercial aluminate powder on lightweight aerated geopolymers. The results showed that MIBA had comparable reaction rate and gas generation capacity to the commercial aluminate powder. Moreover, the resulting MIBA aerated geopolymers had a density of as low as 860 kg/m³ and thermal conductivity of 0.33 W/m·K, which was comparable to the reference aerated geopolymers based on commercial aluminate powder.

On the other hand, several studies have been conducted to use pre-treatments such as alkaline treatment, vitrification, and wet grinding to eliminate the effect of foaming and expansion by metallic aluminate presented in MIBA ([Zhu et al., 2019b](#)). In the series of studies by [Huang et al. \(2019a\)](#), the alkaline treatment was employed. Specifically, MIBA was mixed with sodium hydroxide solution to form slurry and to age this slurry for 4 h, prior to preparing MIBA-based geopolymer composites. Meanwhile, several additives were incorporated during the geopolymer composite preparation for further improving the performance ([Huang et al., 2018b](#); [Huang et al., 2019a, b](#)). The test results showed

that the resulted geopolymer composites possessed satisfactory compressive strength and durability due to the high degree of geopolymerization and dense microstructure (Huang et al., 2018b; Huang et al., 2019b).

More to the point of utilizing MIBA as a precursor or gas-forming additive, researchers have evaluated the feasibility of the application of MIBA to substitute the aggregate in geopolymer composites. The study of Gao et al. (2017) was on this aspect. Here, MIBA was employed as a substitute for a maximum of 50 % fine aggregate (by volume) in geopolymer mortar. Although MIBA negatively affected the strength for its porous and fragile structure, no expansion and cracking was observed due to the metallic aluminate from MIBA. Eventually, the compressive strength of 35–56 MPa can be achieved, suggesting wide application potentials and high reuse rates of MIBA in geopolymer composites. Furthermore, the leaching behavior of formed products met the relevant legislation, confirming the advantages of using geopolymer composites again.

2.1.2. MIFA

MIFA is a fine powder extracted from the combustion gas by the air pollution control devices. Although the weight of MIFA is only 2–5 wt. % of the original MSW before incineration, global MIFA generation is huge and growing up as the increased urbanization and population (Siddique, 2010b). For instance, the quantity of MIFA is estimated to reach 1.0×10^7 tons/year by 2020 in China (Xu et al., 2019). Furthermore, MIFA contains high amounts of heavy metals such as chromium, cadmium, lead, and zinc, etc., and therefore, is considered as hazardous waste (Ashraf et al., 2019). In addition to the heavy metals, several types of soluble salts are the other cause of concern (Siddique, 2010b). Therefore, a method that can attenuate this harm and effectively utilize MIFA is urgently needed.

As geopolymer composites could serve as waste immobilizing agents in the stabilization/solidification (S/S) system of hazardous waste (Ji and Pei, 2019), numerous studies have evaluated the effectiveness of utilizing geopolymers composites for the S/S of MIFA. As shown in Table 1, special attention has been given to the role of synthesis parameters, such as precursor type and content, alkaline activator type and dosage, and curing process, on the S/S efficiency. Overall, geopolymer composites have been proved to be a high-efficiency material for the S/S of MIFA, as such contributing significantly to the reduction in the leachability of toxic elements to the environment. For instance, Lancellotti et al. (2010) incorporated MIFA into the geopolymer matrix based on coal-derived fly ash (CFA). The test results showed that the release of heavy metals from geopolymer composite was much lower with respect to the value of the as-received MIFA, such as the leachable chromium was reduced from 1.57 down to 0.02 mg/L, copper from 3.80 down to 0.04 mg/L, and lead from 11.5 down to 0.1 mg/L. Besides, a recent study demonstrated the excellent long-term S/S efficiency of MIFA-containing geopolymer composites even exposed to the aggressive environment (Jin et al., 2016). Specifically, the leaching concentration of heavy metals (e.g., chromium, copper, lead, zinc, mercury, and cadmium) still remained relatively low after being immersed in aqueous alkali or leached by acid rain. Furthermore, the mechanism of the heavy metal immobilization mechanisms of geopolymer composites containing MIFA has been elucidated by several researchers (Shiota et al., 2017). The mechanism of heavy metals immobilization is believed to perform through both physical and chemical ways, involving the physical encapsulation by the geopolymer matrix, ion exchange of Friedel's salt, and geopolymer adsorption, thus leading that heavy metals are fixed in the geopolymer network (Liu et al., 2019b; Shiota et al., 2017).

The feasibility of MIFA as a precursor in the production of geopolymer composites has also been assessed. Fig. 4 presents the chemical composition of the MIFA from the select studies, which includes the average, minimum, and maximum values, and the XRD pattern of MIFA. In most cases, the low amounts of reactive SiO_2 - and Al_2O_3 -

containing phases presented in MIFA do not allow the formation of chemically stable geopolymer composites without any addition (Tome et al., 2018). Alternatively, the partial replacement of aluminosilicate-rich precursors by MIFA usually resulted in a decrease in mechanical strength (Diaz-Loya et al., 2012; Liu et al., 2019b). Even though the relatively low strength, most resulting products still meet the landfill waste acceptance criteria, further demonstrating the viability of the S/S of MIFA using geopolymer composites before the landfill disposal (Luna Galiano et al., 2011; Ye et al., 2016). However, there also exist studies demonstrating that MIFA exhibited good reactivity in alkaline medium, and thus good mechanical strength for construction purposes (Diaz-Loya et al., 2012; Zhao et al., 2019; Zheng et al., 2016). For instance, compressive strength up to 18.8 MPa at 14 days was obtained in geopolymer pastes based on neat MIFA by Zheng et al. (2016). Diaz-Loya et al. (2012) synthesized geopolymer concrete by the gradual introduction of MIFA to CFA from 20 % to 100 %. The achieved compressive strength and flexural strength varied from 10.1 MPa to 34.3 MPa and from 1.0 MPa to 3.5 MPa, respectively, after curing for 7 days at 100 °C.

As the contents of chlorides and sulfates are commonly high in MIFA (as shown in Fig. 4), the negative effects of these compounds on geopolymerization kinetic cannot be ignored. Zheng et al. (2011) utilized the water-wash pre-treatment to eliminate the inorganic salt from MIFA and then investigated the geopolymerization of MIFA to determine the efficacy of water-wash pre-treatment. It was found that water-wash pre-treatment considerably promoted the early strength and also resulted in a higher ultimate strength (22.7 MPa at 28 days) in comparison with the counterpart without water-wash pre-treatment. Meanwhile, a better immobilization efficiency of heavy metal was identified in the geopolymer composites based on water-washed MIFA. Therefore, a viable and practical pre-treatment is essential for the use of MIFA as the raw material for geopolymer composites in civil construction applications as well as a more effective stabilization process.

2.2. Waste paper

By far, the application of raw waste paper in construction materials is not very common. Instead, a large quantity of waste paper has been recycled into new paper products, which could conserve wood and other forest resources, and make less environmental impacts. However, the processing of recycled paper into usable fiber for papermaking often generates a secondary stream typically termed as waste paper sludge. This sludge has a high content of water ranging from 50 % to 70 % and therefore is usually dried before processing for ease handling, incineration, and any potential applications. Besides, waste paper sludge contains approximately equal amounts of organics (mainly residual cellulose fiber) and inorganic fillers (such as kaolin clay and calcium carbonate) (Kinuthia, 2018). Previous studies mainly focused on employing waste paper sludge in the construction materials based on OPC, while the utilization of waste paper sludge in geopolymer composites is a relatively advanced development (Yan and Sagoe-Crentsil, 2012).

In general, the studies on the utilization of waste paper sludge in geopolymer composites show two main approaches. Chemical analysis has indicated that waste paper sludge appears compatible with geopolymer chemistry, and could serve as a potential supplementary additive to geopolymer composites. Thus, the first approach adopts this material in its raw form. Yan and Sagoe-Crentsil (2012) evaluated both fresh and hardened properties for the geopolymer mortar incorporating 2.5–10 % dry waste paper sludge by weight of total precursor. Results demonstrated that the incorporation of waste paper sludge into geopolymer mortar reduced the workability by 11–33 % and decreased compressive strength by 8–42 %. However, the compressive strength still maintained over 31.2 MPa. It was also reported that, with increasing waste paper sludge addition, the geopolymer drying shrinkage was decreased by up to 64 %, which was contrary to the trend of increasing drying shrinkage observed for the OPC matrix after the

Table 1
The recent research on the applications of MIFA in geopolymer composites.

Precursor ¹	Activator	Curing condition ²	MIFA content	Leachate analysis ³	Compressive strength	Reference
Blend with aluminosilicate-rich precursors						
Uncalcined coal gangue	NaOH + Na ₂ SiO ₃	30, 45, 60, 75 or 90 °C for 24 hrs	10–60 %	Cu, Zn, Pb, and Cd	1.7–28.7 MPa (7 days) 2.1–31.4 MPa (28 days)	Zhao et al. (2019)
GGBFS and CFA	NaOH + Na ₂ SiO ₃	RT	20–40 %	Cu, Zn, Pb, Cr, Ba, Se	Grate-firing bed MIFA: 11.7–20.2 MPa (28 days) Fluidized bed MIFA: 28.7–36.7 MPa (28 days)	Xu et al. (2019)
Granulated lead smelting slag	NaOH + Na ₂ SiO ₃	RT	20–80 %	Zn, Pb, As, Cd, Ni, Cr, Ba, and Cu	5.1–12.5 MPa (7 days) 5.4–15.3 MPa (28 days)	Liu et al. (2019b)
Red mud	NaOH + Na ₂ SiO ₃	RT	20–50 %	Zn, Pb, As, Cd, Ni, Cr, Ba, Be, Cu, Se, Sb, Co, and V	—	Li et al. (2019)
Volcanic ash	NaOH + Na ₂ SiO ₃	RT	50–100 %	Zn, Cr, Hg, Zn, Ba, Se, Ag, and Cd	1.1–7.2 MPa (7 days) 1.4–10.5 MPa (28 days)	Tome et al. (2018)
Dehydrated pyrophyllite	NaOH + Na ₂ SiO ₃	60, 80, and 105 °C for 34 hrs	50 %	Cs	1.4–3.9 MPa (7 days)	Shiota et al. (2017)
Bayer red mud	NaOH	RT	40–60 %	Cu, Zn, Pb, and Cr	1.2–1.7 MPa (28 days)	Ye et al. (2016)
MK	NaOH + Na ₂ SiO ₃	RT	40 %	Pb, Zn, Cu, Cr, Cd, and Hg	36.1 MPa (28 days)	Jin et al. (2016)
CFA	NaOH + Na ₂ SiO ₃	100 °C for 7 days	20–100 %	Pb, As, Cd, Cr, Ba, Se, Ag, and Hg	10.1–34.3 MPa (7 days)	Diaz-Loya et al. (2012)
CFA, GGBFS, kaolin, and MK	NaOH + Na ₂ SiO ₃ ; KOH + K ₂ SiO ₃	RT, and 60 °C for 7 days	23–26 %	Pb, Cd, Cr, Zn and Ba	1–3 MPa (7 days)	Luna Galiano et al. (2011)
MK	NaOH + Na ₂ SiO ₃	50 °C for 24 hrs	17 %	Cr, Cd, Ni, Cu, and Pb	1–9 MPa (7 days)	Lancellotti et al. (2010)
Use as a neat precursor						
MIFA	NaOH; NaAlO ₂ ; Na ₂ SiO ₃	RT	100 %	Cu, Zn, Pb, and Cd	7.1–18.8 MPa (14 days)	Zheng et al. (2016)
MIFA	NaOH + Na ₂ SiO ₃	RT	100 %	Cr, Cu, and Zn	Unwashed MIFA: 15.9 MPa (28 days) Water-washed MIFA: 22.7 MPa (28 days)	Zheng et al. (2011)

Note: 1. GGBFS, CFA, and MK denote ground granulated blast furnace slag, coal-derived fly ash, and metakaolin, respectively; 2. RT represents room temperature; 3. Ag–silver, As–arsenic, Ba–barium, Be–beryllium, Cd–cadmium, Co–cobalt, Cr–chromium, Cs–cesium, Cu–copper, Hg–mercury, Ni–nickel, Pb–lead, Se–selenium, Sb–antimony, V–vanadium, Zn–zinc.

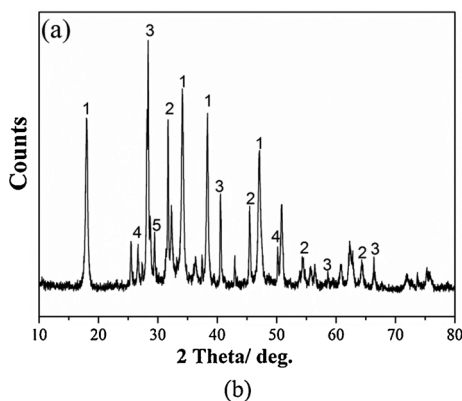
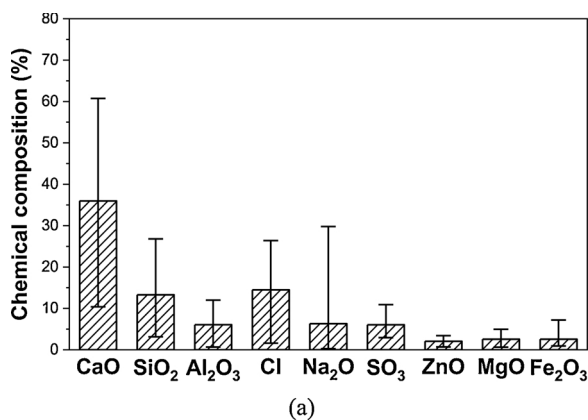


Fig. 4. Chemical composition and mineralogy of MIFA: (a) Chemical composition of MIFA from the selected studies. Data from Diaz-Loya et al. (2012); Jin et al. (2016); Lancellotti et al. (2010); Li et al. (2019); Liu et al. (2019b); Luna Galiano et al. (2011); Tome et al. (2018); Xu et al. (2019); Ye et al. (2016); Zhao et al. (2019); Zheng et al. (2011), 2016; (b) XRD pattern of MIFA (1, CaClOH; 2, NaCl; 3, KCl; 4, SiO₂; 5, CaCO₃) (Li et al., 2019).

inclusion of waste paper sludge.

More recently, Adesanya et al. (2018) utilized waste paper sludge as a waste-based source of calcium carbonate in the one-part (“just add water”) geopolymer. Specifically, waste paper sludge was pre-treated by mixing with sodium hydroxide and then dried in the oven, in which waste paper sludge acted as activator and also as filler. The test results showed that the generated geopolymer mortar possessed the compressive strength up to 48 MPa at 50 days. In addition, the prepared sample exhibited low drying shrinkage, with the highest shrinkage of 0.39 % and the lowest of 0.14 % at 90 days.

The other approach of recycling waste paper sludge in geopolymer composites is the use of waste paper sludge ash (WPSA), which derives from the thermal processes such as the combustion of waste paper sludge. During the combustion process, the latent energy of the organic component can be recovered. At the same time, the highly reactive metakaolin-type phases and calcined limestone are produced (Antunes Boca Santa et al., 2013). The chemical composition and mineralogy of WPSA from the selected studies are presented in Fig. 5. It was found that WPSA can be utilized as a precursor substitution in geopolymer composites (Antunes Boca Santa et al., 2013; Mamat et al., 2018; Yan and Sagoe-Crentsil, 2016). Fig. 6 presents the relationship between the inclusion percentage of WPSA and the relative compressive strength. Although the inclusion of WPSA has varied effects in different studies owing to the different raw materials and curing conditions, these results consistently indicated that the inclusion of WPSA in geopolymer composites presented a positive effect on the degree of geopolymerization and therefore resulted in better mechanical performance. Moreover, some researchers investigated the geopolymer composites based on

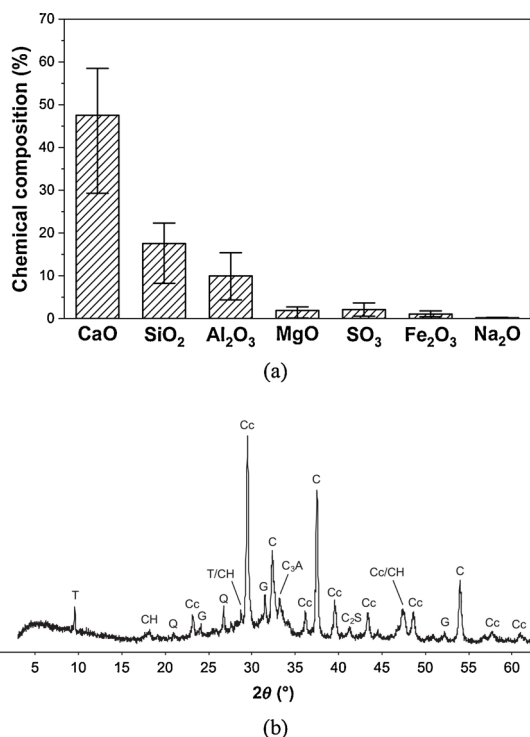


Fig. 5. Chemical composition and mineralogy of WPSA: (a) Chemical composition of WPSA from the selected studies. Data from Bernal et al. (2014); Gluth et al. (2014); Mamat et al. (2018); Ridzuan et al. (2014b); Yan and Sagoe-Crentsil (2016); (b) XRD pattern of WPSA (CH: portlandite, Q: quartz, Cc: calcite, G: gehlenite, C: lime, C₃A: tricalcium aluminate, C₂S: belite) (Gluth et al., 2014).

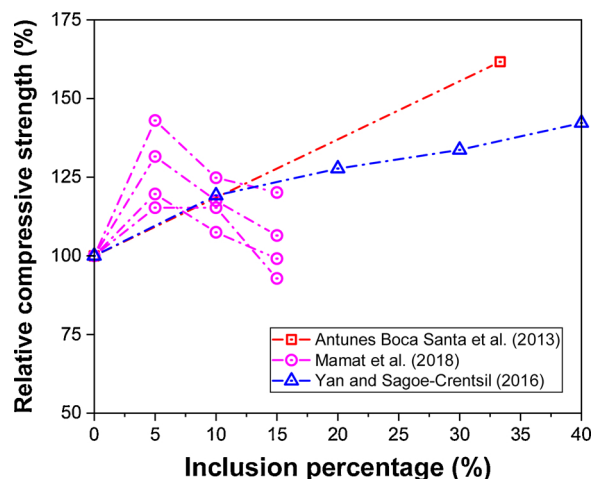


Fig. 6. Relationship between the inclusion percentage of WPSA and relative compressive strength (Antunes Boca Santa et al., 2013; Mamat et al., 2018; Yan and Sagoe-Crentsil, 2016).

WPSA only (Bernal et al., 2014; Gluth et al., 2014; Ridzuan et al., 2014a). It was elucidated that WPSA was a suitable precursor for producing geopolymer composites (Gluth et al., 2014), and also the formulation parameters, especially the concentration of alkaline activators, need to be optimized to manufacture a desirable product (Bernal et al., 2014; Ridzuan et al., 2014b).

2.3. Rubber waste

Enormous disposal of rubber waste has become a challenging task, as rubber, featured with a three-dimensional network structure, takes a

Table 2
Recent research on the applications of rubber waste in geopolymer composites.

Composites	Form	Substitution	Content ¹	Precursor	Activator	Curing condition	Mechanical properties ²	Reference
Concrete	Rubber fiber (width: 2–4 mm; length: 22 mm)	Fine aggregate	0, 10, 20, and 30 wt. %	CFA	NaOH + Na ₂ SiO ₃	90 °C for 48 hrs	30.0–48.3 MPa (28-day compressive strength) 8.4–8.8 MPa (28-day flexural strength)	Luhar et al. (2018, 2019a, 2019b, 2019c, 2019d)
		Crumb rubber	0, 5, 10, 15, and 20 wt.%	CFA	NaOH + Na ₂ SiO ₃	RT	5.1–5.3 MPa (28-day indirect tensile strength) 11.3–33.2 MPa (28-day compressive strength)	Azmi et al. (2019)
		Crumb rubber (0–4 mm)	0, 10, 20, and 30 vol %	GGBFS	NaOH + Na ₂ SiO ₃	RT	24.6–40.0 MPa (28-day compressive strength) 1.8–2.0 MPa (60-day flexural strength)	Aly et al. (2019)
		Crumb rubber (5–10 mm)	0, 5, 10, 15, and 20 wt.%	CFA	NaOH + Na ₂ SiO ₃	Seawater	2.3–2.8 MPa (60-day indirect tensile strength)	Yahya et al. (2018)
		Crumb rubber (0–3.75 mm)	0, 5, 10, 15, 20 wt.%	CFA	NaOH + Na ₂ SiO ₃	RT	14.1–40.0 MPa (28-day compressive strength)	Azmi et al. (2016)
Mortar	Crumb rubber (0–4.75 mm)	Fine aggregate	0, 5, 10, 15, and 20 vol%	CFA	NaOH + Na ₂ SiO ₃	46 °C for 7 days (stream-curing)	17.5–40.6 MPa (7-day compressive strength)	Park et al. (2016)
		Fine aggregate	0, 2, 6, 10, and 14 wt. %	MK	NaOH + Na ₂ SiO ₃	65 °C for 48 hrs	9.0–42.9 MPa (28-day compressive strength)	Gandoman and Kokabi (2015)
		Fine aggregate	0, 5, 10, and 15 wt.%	CFA + GGBFS	NaOH + Na ₂ SiO ₃	RT	30.9–35.6 MPa (28-day compressive strength)	Zhong et al. (2019)
		Fine aggregate	0, 5, 10, and 15 wt.%	CFA + GGBFS	NaOH + Na ₂ SiO ₃	RT	3.6–3.9 MPa (28-day flexural strength)	
		Fine aggregate	0 and 100 vol%	CFA	NaOH + Na ₂ SiO ₃	25, 60, 90 °C for 48 hrs	2.7 MPa (28-day compressive strength)	Wongsa et al. (2018a)
Crumb rubber (0–4.25 mm)	Fine aggregate	100 vol%	CFA	NaOH + Na ₂ SiO ₃	RT	1.0 MPa (28-day flexural strength)		S. Mohammed et al. (2018)
	Fine aggregate	0, 20, 40, and 60 vol%	GGBFS	NaOH + Na ₂ SiO ₃	RT	2.8–4.3 MPa (28-day compressive strength)		Long et al. (2018)
	Fine aggregate	0, 20, 40, and 60 vol%	GGBFS	NaOH + Na ₂ SiO ₃	RT	14.6–31.3 MPa (28-day compressive strength) 8.6–14.7 MPa (28-day flexural strength)		

Note: 1. wt.% and vol% denote the replacement percentages by weight and volume, respectively; 2. The mechanical properties exclude the results of control specimens (the specimens without rubber waste).

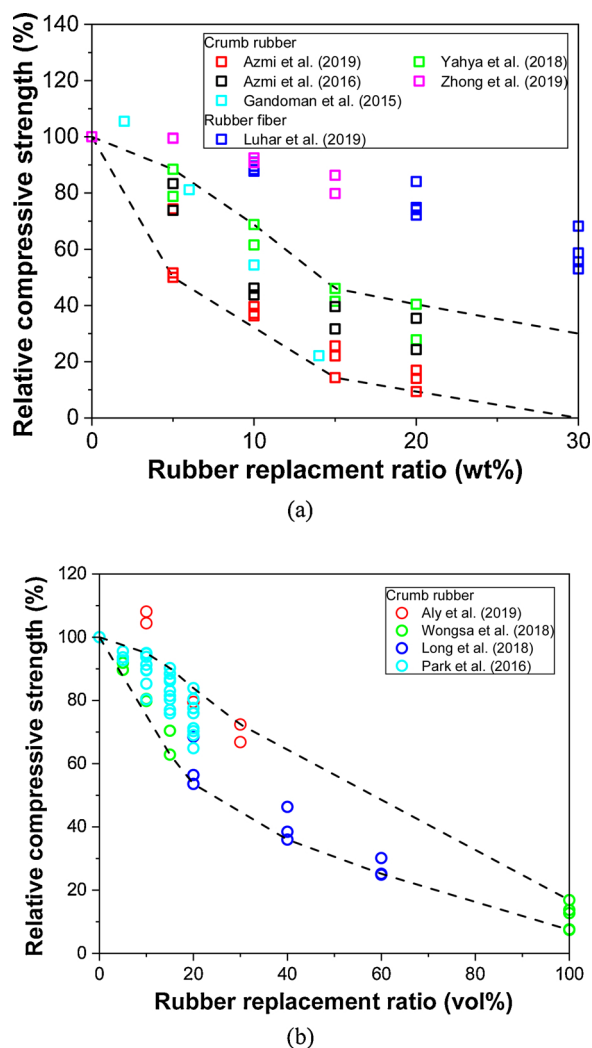


Fig. 7. Relationship between the replacement ratio of waste rubber and relative compressive strength: (a) Replacement by mass; (b) Replacement by volume.

very long time to decompose. The waste tire is by far the predominant source of rubber waste, and it is estimated to exceed 200 million annually by 2030 (Thomas and Gupta, 2016). The traditional method of waste tire management includes stockpiling or dumping and landfilling, all of which are a short-term solution. Moreover, stockpiled tires could provide favorable breeding grounds for insects and mosquitoes. It would also cause an environmental impact as the toxins in tires can easily leach out, thus causing the contamination to the soil and groundwater. Henceforth, recycling these waste tires is an urgent environmental task worldwide. The use of rubber waste, recycled from automotive and truck scrap tires, in geopolymer composites was introduced in recent years (Gandoman and Kokabi, 2015). The existing studies are summarized in Table 2.

The most preferred method for the recycling of tire rubber is grinding shredded tire pieces into granules with desired sizes, namely, crumb rubber. When used in geopolymer composites, the crumb rubber replaces coarse or fine aggregates partially or even fully. There is a consensus among the existing studies that the addition of crumb rubber into geopolymer composites remarkably alters the properties of geopolymer composites. As illustrated in Fig. 7, the compressive strength showed a systematic reduction with the increment of the crumb rubber replacement ratio. Also, the loss of strength due to crumb rubber substitution by mass replacement is greater than that by volume replacement under a certain percentage. The loss of strength can be explained from several aspects. One of the main reasons is the hydrophobic nature

of rubber, which causes the weak bond between the rubber and geopolymer matrix. Long et al. (2018) performed a microstructure test and confirmed the imperfect adhesion between the rubber aggregates and the geopolymer matrix, which was indicated by the deep cracks and voids at the interface. Another cause of the strength loss is the significantly low modulus of rubber, which could result in the premature cracking near the joint of the rubber and geopolymer matrix. However, an insignificant reduction of the mechanical strength can be obtained if the rubber replacement ratio within an appropriate amount, which therefore is suitable for structural purposes (Park et al., 2016; Wongsa et al., 2018a; Yahya et al., 2018). Otherwise, geopolymer composites with high replacement ratios are limited to secondary or non-critical structures, similar to the study of S Mohammed et al. (2018), that the non-load bearing brick was developed by utilizing crumb rubber as the sole fine aggregate in the geopolymer mortar. Analogously, degradation was also observed for other mechanical performance, physical properties, and durability by the crumb rubber incorporation. Recently, the study of Zhong et al. (2019) disclosed that the comparable compressive (as shown in Fig. 7(a)) and superior flexural strength could be achieved in waste rubber geopolymer composites by introducing steel fibers. That is, the incorporation of steel fibers into geopolymer composites could compensate for the strength loss caused by crumb rubber while maintaining its positive impact. As a result, the usage of rubber waste in geopolymer composites can be maximized.

Fig. 7 also demonstrates that the replacement of rubber waste in the form of rubber fiber has less effect on the compressive strength than that in the form of crumb rubber (Luhar et al., 2019a). Additionally, rubber fiber was found to improve the tension properties of geopolymer concrete, such as flexural strength and splitting tensile strength, with the increased percentage of rubber fiber. For example, Luhar et al. (2019a) reported that, at 28 days, the splitting tensile strength and flexural strength were improved from 5.0 MPa to 5.3 MPa, and from 6.4 MPa to 6.8 MPa, respectively, after 30 % replacement of fine aggregate by rubber fibers. This improvement was associated with that the fibers could provide a bridge between propagated cracks.

On the other hand, Aly et al. (2019) investigated the impact resistance of geopolymer composites with three different levels of aggregate replacement by crumb rubber under drop weight test. Based on the test results, improved impact energy absorption was observed in geopolymer composites with higher contents of crumb rubber. It can be explained by that rubber possesses good elastic behavior especially at large deformation, and good energy absorbing capacity. In other words, rubber can absorb sudden shock as its nature, which cannot be achieved by natural aggregates due to the brittle nature. The inclusion of crumb rubber was also found to enhance the viscoelasticity and the damping properties of the geopolymer mortars. The study by Long et al. (2018) reported that the damping ratio of geopolymer mortar increased dramatically after the inclusion of crumb rubber, rising from 0.05 to 0.12.

In addition, the enhanced insulation properties (acoustic impedance and thermal conductivity) have been reported for geopolymer composites containing crumb rubber (Gandoman and Kokabi, 2015; Wongsa et al., 2018a). As reported, the thermal conductivity of geopolymer concrete was greatly lowered by the incorporation of crumb rubber, decreasing from 1.284 W/mK to 0.237 W/mK (Wongsa et al., 2018a). It is due to that rubber has lower thermal conductivity, ranging from 0.1 W/mK to 0.25 W/mK, in comparison with the thermal conductivity of normal aggregate, approximately 1.5 W/mK. Gandoman and Kokabi (2015) compared the sound transmission loss and sound absorption of geopolymer concretes with varied waste rubber content, under different ranges of sound frequencies. Test results validated the pronounced improvement in noise reduction coefficient and sound absorption property for geopolymer concrete after the inclusion of crumb rubber.

2.4. Plastic waste

Plastic waste has become one of the most pressing environmental

issues, as the rapidly increasing production of plastic products overwhelms the world's ability to deal with them. It is well known that plastic is a non-biodegradable material that takes a long time to break down when it is landfilled, and thus landfilling plastic products poses a heavy burden on the environment. In addition, since plastics production involves the use of some harmful chemicals, land-filling plastic waste would result in the release of harmful chemicals. One of the best solutions to reduce these negative effects is to recycle plastic waste to produce new materials such as mortar or concrete (Saikia and de Brito, 2012).

Several works have been carried out to evaluate the properties of geopolymer composites containing plastic waste as aggregate. In the study by Wongkvanklom et al. (2019), the plastic waste was melted to form lumps and then ground into particles with a diameter of about 2.1 mm to act as fine aggregate for the geopolymer composite preparation. Akçaözoglu and Ulu (2014) substituted the waste PET bottles granules, having particle sizes less than 4 mm, for the fine aggregates in geopolymer mortar at different levels (20–100 %). Besides, Posi et al. (2015) incorporated the polystyrene foam particles with a size between 2.36 mm and 4.75 mm, which was sourced from the discarded packaging foam, into geopolymer concrete. Generally, the density of geopolymer composites decreased with the increase of replacement ratios of waste plastic aggregate, mainly attributing to the low density of plastic material. The increasing of waste plastic aggregate replacing ratios also resulted in the decreases in mechanical properties, including compressive strength and flexural strength, as shown in Fig. 8. However, the waste plastic aggregate replacement under an appropriate ratio could produce geopolymer concrete with acceptable strength and density to serve as an alternative to lightweight structural concrete (Posi et al., 2015). In addition, the reduction in the surface abrasion resistance, and increase in the porosity and water absorption were also observed as the amount of waste plastic aggregate increased (Wongkvanklom et al., 2019). Due to the low thermal conductivity coefficient of plastic, the inclusion of plastic waste additionally equips geopolymer composites with lower thermal conductivity and better thermal insulation properties (Posi et al., 2015).

In another study, Dave et al. (2017) replaced the virgin coarse aggregate by waste plastic granules with the diameters of between 7 mm and 9 mm in geopolymer concrete, and then investigated the impact resistance of geopolymer concrete by performing drop hammer test. The test results revealed that the 10 % inclusion of waste plastic aggregate greatly improved the impact resistance from 179.77 kJ to 193.02 kJ. It has been explained that the plastic aggregate possessed excellent ductile properties that could well absorb sudden impact energy, and thus arrested the cracks propagation at the micro level.

Inspired by the successful employment of plastic waste fiber as one constituent in OPC based concrete, researchers examined its feasibility in geopolymer composites (Bhogayata and Arora, 2019; Patel et al., 2013). As expected, plastic waste could be successfully utilized in the formulation of geopolymer composites as reinforcement fiber. For instance, Bhogayata and Arora (2019) mixed the plastic waste fiber (with average size of 20 mm length and 1 mm width) in geopolymer concrete under varying proportions from 0% to 2% by volume. The plastic waste fiber was obtained from shredding the metalized plastic films, which is the polypropylene-based metalized thin film with a layer of aluminum on one side surface and usually used as a food package. It was identified that the addition of plastic waste fiber reduced the workability, density, and compressive strength of geopolymer concrete. While as for the splitting tensile strength, it was increased by about 8%, 18%, 16%, and 12% for the increment of the plastic waste fiber dosage from 0.5% to 2%. Furthermore, the enhancement was also observed in the strength and deformation capacity under flexural loading, as well as the energy absorption under the impact.

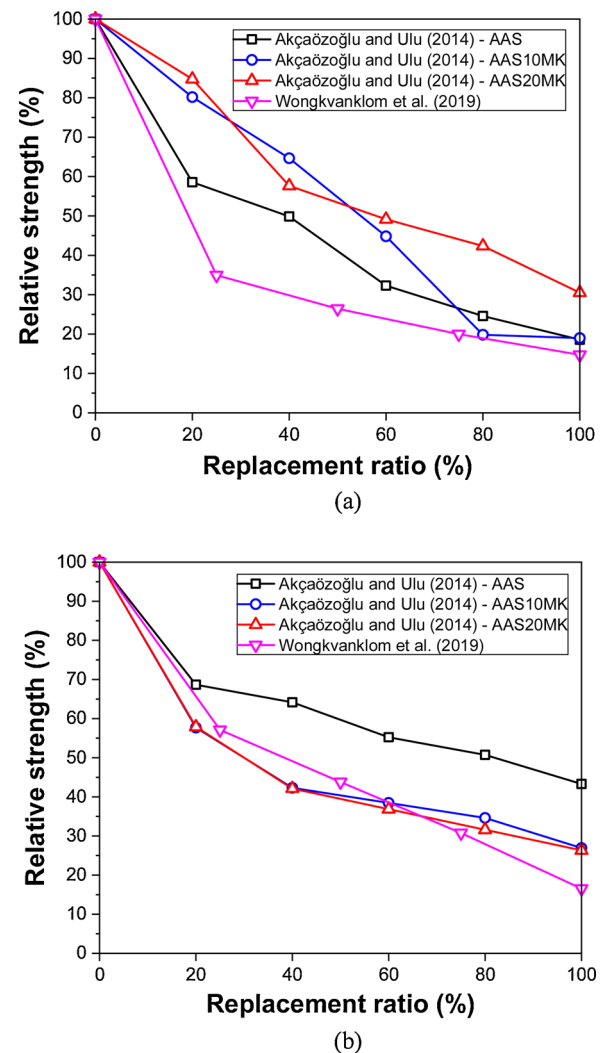


Fig. 8. Relationship between the replacement ratio of waste plastic and relative strength: (a) Compressive strength; (b) Flexural strength.

2.5. Other wastes

2.5.1. Waste glass

In addition to the above-discussed MSW, other types of MSW have achieved varied progress in the re-utilization in geopolymer composites. One of the predominant is that in reusing glass waste. The global annual generation of glass waste is about 65 million tons, accounting for about 5% of the MSW composition (Hoornweg and Bhada-Tata, 2012). Nevertheless, waste glass has not been fully recycled or efficiently reused. In the United States, only 28 % of waste glass was recycled from 11.54 million tons. In Mainland China, 40 million tons of waste glass is produced annually, but with only 13 % of it being recycled (Liu et al., 2019c). The chemical composition and mineralogy of glass is given in Fig. 9. It contains abundant amorphous silicon and calcium, and also has high reactivity. The suitability of employing waste glass in manufacturing geopolymer composites has been verified by extensive researches. In general, glass waste could be re-utilized as aggregates (Hajimohammadi et al., 2018; Lu and Poon, 2018), precursors (Si et al., 2020; Xuan et al., 2019), and alkali activators (Vinai and Soutsos, 2019), in the context of geopolymer. Since there are several studies that have reviewed the reuse of glass waste in geopolymer composites, researchers attempting to valorize the glass waste through the development of geopolymer composites can consult these fruits (Liu et al., 2019c; Luhar et al., 2019c, d; Moghadam et al., 2019).

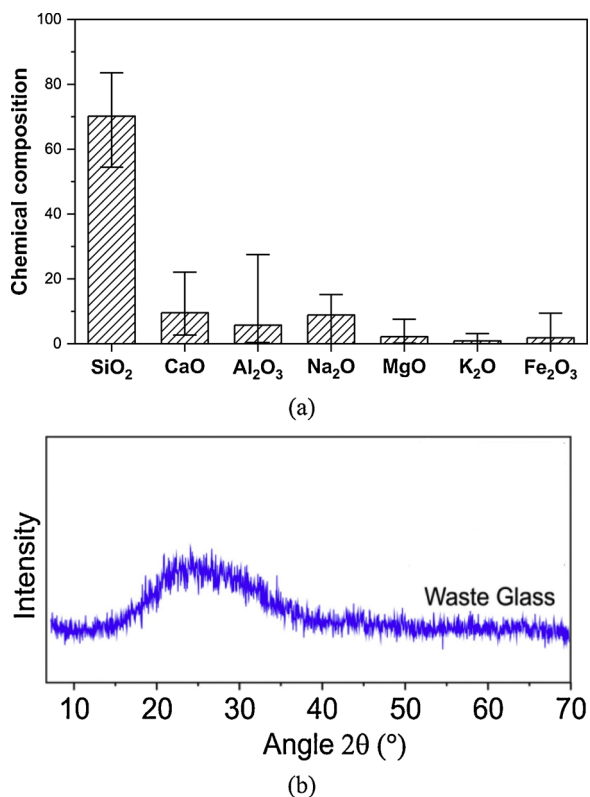


Fig. 9. Chemical composition and mineralogy of waste glass: (a) Chemical composition of waste glass (Liu, Y. et al., 2019); (b) XRD pattern of waste glass (Q: Quartz) (Burciaga-Díaz et al., 2020).

2.5.2. Tire steel and textile fiber

During the process of grinding tires into granules, steel and textile waste are also obtained. The possibility of using these materials recovered from tires as fiber reinforcement for geopolymer composites has been examined (Łach et al., 2018; Onuaguluchi et al., 2017; Zhong et al., 2019). It has been demonstrated that although the tire steel fiber might impair the compressive strength, a remarkable enhancement in flexural performance was observed for geopolymer composites reinforced with tire steel fiber. For example, Onuaguluchi et al. (2017) reported that the addition of 1% and 2% tire steel fiber increased the flexural peak strength by 71.5 % and 45.1 %, respectively; and increased the toughness from 0.14 J to 1.70 J and 2.18 J, respectively. Similar results have also been identified in the geopolymer composites reinforced with tire textile fiber (Łach et al., 2018). Specifically, the

introduction of tire textile fiber altered the failure mode from brittle to ductile, and the flexural strength was improved by up to 10 % due to the inclusion of tire textile fiber.

2.5.3. Spent coffee grounds

Spent coffee grounds are the solid granular residue of the ground beans during the final liquid coffee making, and are primarily disposed to landfills. A series of studies have been conducted to assess the feasibility of combining coffee grounds with geopolymer precursors into sustainable subgrade construction materials (Arulrajah et al., 2017; Kua et al., 2017, 2018; Suksiripattanapong et al., 2017). Specifically, coffee grounds, used as the fill materials, were blended with a controlled ratio of geopolymer precursors (e.g., CFA, slag, or even glass waste), and then activated with an alkali solution. The performance of the produced materials was examined in terms of compressive strength, elastic modulus, microstructure properties, and contaminants leaching. On the whole, the test results revealed that geopolymers could be employed to stabilize coffee grounds into a subgrade material meeting the strength, stiffness, and environmental requirements.

2.5.4. Waste cork

In the investigation by Novais et al. (2019), the pyrolyzed waste cork was, for the first time, used to synthesize the geopolymer-cork composites. Recycled corks, sourced from wine stopper, were heated to 900 °C under nitrogen in a graphite furnace, followed by being ground into powder below 75 μm. The addition of 2.5 % and 3.75 % pyrolyzed cork was directly added to the geopolymer composites. Due to the high carbon content (90.74 wt.%), pyrolyzed cork could act as a carbon source to enhance geopolymer composites' electromagnetic interference shielding properties. Results exhibited that all cork-geopolymer composites presented enhanced specific shielding effectiveness in comparison with the normal geopolymer matrix. Taking the samples with 3 mm thickness for instance, the specific shielding effectiveness was increased from 4.7 to 6.0 -dB g⁻¹ cm³ to 8.8–10.8 and 11.7–13.5 -dB g⁻¹ cm³, respectively, after the addition of 2.5 % and 3.75 % pyrolyzed cork. Overall, the incorporation of pyrolyzed cork into geopolymer composites provided an environmentally friendlier strategy for electromagnetic interference shielding applications.

3. Construction solid waste

Construction solid waste (CSW), an inescapable by-product of the construction, renovation, or demolition activities, comprises a wide array of materials, including concrete, metals, bricks, timber, ceramics, asphalt, soil, plaster and polymers. This waste accounts for the largest source of the solid waste stream in most countries around the world. Fig. 10 gives the annual CSW generation from the selected countries in

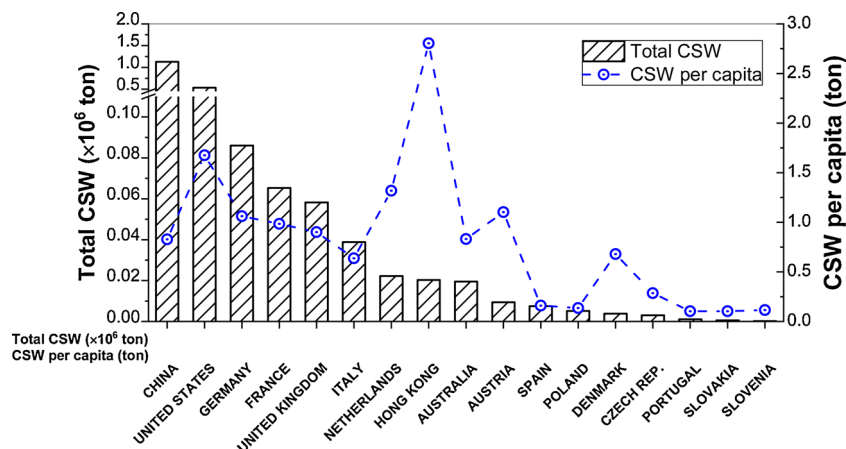


Fig. 10. Annual CSW generation from selected countries (Menegaki and Damigos, 2018).

Table 3
Recent research on the applications of recycled concrete aggregate in geopolymer composites.

Composites	Size (mm)	Substitution	Content (wt.%)	Precursor ¹	Activator	Curing condition	Mechanical properties ²	Variation in durability ³	Reference
Concrete	5-20	Coarse aggregate	0, 50, 100	CFA	NaOH + Na ₂ SiO ₃	RT	54.7–71.6 MPa (28-day compressive strength)	—	Shi et al. (2012)
	4.5–9.5	Coarse aggregate	0, 100	CFA	NaOH + Na ₂ SiO ₃	60 C for 48 h	7.0–10.3 MPa (7-day compressive strength) 1.3–1.5 MPa (7-day indirect tensile strength)	Increase by 24 % (Permeability depth)	Sata et al. (2013)
	5-16	Coarse aggregate	0, 25, 50, 75, 100	GBBFS	NaOH + Na ₂ SiO ₃	RT	52.2–56.5 MPa (28-day compressive strength) 4.3–4.7 MPa (28-day indirect tensile strength) 4.6–5.3 MPa (28-day flexural strength)	Increase by 53–184 % (Chloride penetration) Increase by 13–135 % (Sulphate corrosion)	Kathirvel and Kaliyaperumal (2016, 2017) Liu et al. (2016)
	0-20	Aggregates	100	CFA	NaOH + Na ₂ SiO ₃	RT	18.0–27.2 MPa (Compression)	—	
	4.5–9.5	Coarse aggregate	0, 100	CFA	NaOH + Na ₂ SiO ₃	60 C for 48 h	30.6–38.4 MPa (28-day compressive strength) 2.9–4.0 MPa (28-day indirect tensile strength) 4.0–5.3 MPa (28-day flexural strength)	Increase by 3–64 % (Chloride penetration) Increase by 4–97 % (Acid corrosion)	Nuaklong et al. (2016)
	4.75-11.8	Coarse aggregate	100	CFA + OPC	NaOH + Na ₂ SiO ₃	25, 40, 60 and 90 C	4.5–17.5 MPa (Compression)	—	Posi et al. (2016)
	4.75-9.5	Coarse aggregate	0, 10, 20, 30, 40, 50, 80, 100	CFA	NaOH + Na ₂ SiO ₃	75 C for 48 h	43.5–54.7 MPa (28-day compressive strength)	—	Samusi et al. (2016)
	0-20	Coarse aggregate	0, 15, 30, 50	CFA	NaOH + Na ₂ SiO ₃	60 C for 24 h	36.8–41.8 MPa (28-day compressive strength) 3.0–3.7 MPa (28-day indirect tensile strength) 14–20 GPa (28-day elastic modulus)	Increase by 68–129 % (Chloride penetration)	Shaikh (2016)
	4.5–9.5	Coarse aggregate	0, 100	CFA + MK	NaOH + Na ₂ SiO ₃	60 C for 48 h	32.9–47.2 MPa (28-day compressive strength) 2.7–3.5 MPa (28-day indirect tensile strength) 3.6–6.0 MPa (28-day flexural strength)	Increase by 2–11 % (Surface abrasion) Increase by 16–83 % (Acid corrosion) Increase by 9–15 % (Chloride penetration)	Nuaklong et al. (2018a)
	4.5–9.5	Coarse aggregate	0, 100	CFA + OPC/nS	NaOH + Na ₂ SiO ₃	60 C for 48 h	31.6–48.7 MPa (28-day compressive strength) 2.6–3.0 MPa (28-day indirect tensile strength) 3.6–4.4 MPa (28-day flexural strength)	Increase by 47–218 % (Chloride penetration) Increase by 53–74 % (Acid corrosion)	Nuaklong et al. (2018b)
	2-19	Coarse aggregate	100	CFA + GGBFS	NaOH + Na ₂ SiO ₃	80 C for 24 h	25.2–79.6 MPa (28-day compressive strength) 12.3–23.1 GPa (28-day elastic modulus)	—	Xie et al. (2018)
	5-20	Coarse aggregate	0, 50, 100	CFA + GGBFS	NaOH + Na ₂ SiO ₃	75 C for 24 h	13.7–43.0 MPa (28-day compressive strength) 1.6–4.2 MPa (28-day indirect tensile strength) 2.2–4.4 MPa (28-day flexural strength)	—	Hu et al. (2019); Tang et al. (2019a)
	—	Coarse aggregate	0, 10, 20, 30	MK	NaOH + Na ₂ SiO ₃	RT	9.6–18.0 GPa (28-day elastic modulus) 27.8–40.9 MPa (90-day compressive strength)	Increase by 6–67 % (Chloride penetration)	Koushkbaghi et al. (2019)
	5-40	Coarse aggregate	0, 30, 50, 70, 100	CG + GGBFS + CAF	NaOH + Na ₂ SiO ₃	60 C	23.6–29.4 MPa (28-day compressive strength) 1.3–2.7 MPa (28-day indirect tensile strength)	—	Liu et al. (2019a)
	5-20	Coarse aggregate	0, 50, 100	CFA + GGBFS	NaOH + Na ₂ SiO ₃	80 C for 24 h	37.1–47.7 MPa (28-day compressive strength) 11.5–16.3 GPa (28-day elastic modulus)	—	Xie et al. (2019a)
	5-20	Coarse aggregate	0, 30, 50, 70, 100	CFA + GGBFS	NaOH + Na ₂ SiO ₃	80 C for 24 h	40.9–61.9 MPa (28-day compressive strength) 12.4–22.1 GPa (28-day elastic modulus)	—	Xie et al. (2019b)
Mortar	2-9	Fine aggregate	0, 25, 50	GBBFS	NaOH + Na ₂ SiO ₃	RT	54.5–56.7 MPa (28-day compressive strength)	Decrease by 25–37 % (91-day autogenous shrinkage)	Lee et al. (2018)
	0-4	Fine aggregate	0, 100	SiMn slag	NaOH, NaOH + Na ₂ SiO ₃	RT	11.6–33.8 MPa (28-day compressive strength)	Decrease by 12–22 % (91-day drying shrinkage) Increase by 59–119 % (147-day autogenous shrinkage)	Navarro et al. (2018)
	0-5	Fine aggregate	0, 25, 50, 75, 100	GBBFS	NaOH + Na ₂ SiO ₃	RT	0–5 MPa (28-day flexural strength)	Decrease by 26–43 % (147-day drying shrinkage)	
	0.5-2.0	Fine aggregate	0, 100	CFA + MK	NaOH + Na ₂ SiO ₃	RT	55.7–62.6 MPa (28-day compressive strength) 22.8–26.4 MPa (28-day compressive strength) 2.2–5.3 MPa (28-day flexural strength)	Increase by 35–40 % (residual strength after elevated temperatures)	Sedaghatdoost et al. (2019) De Rossi et al. (2019)

Note: 1. CG, nS, SiMn denote coal gangue and nano-SiO₂, silico-manganese, respectively; 2. The mechanical properties exclude the results of control specimens (the specimens without recycled aggregates); 3. The positive value means the reverse trend.

2014 (Menegaki and Damigos, 2018). As a result, how to address the CSW problem has raised great concerns from economic, environmental, and societal perspectives. In recent decades, numerous studies have been devoted to increasing the recycling rate and reducing landfill rate of CSW. This section provides a thorough review of the achievement in recycling CSW in geopolymer composites, including waste concrete, waste clay brick, ceramic waste, and waste asphalt pavement, along with some others.

3.1. Concrete waste

Concrete is the most widely used building material as its relatively low cost, availability of raw materials, and good mechanical and durability properties. Accordingly, it has been reported that approximately one-third of CSW consists of concrete. The waste concrete was once routinely trucked to landfills for disposal, but recycling has plentiful benefits that make it an attractive alternative in this age of more environmental laws, greater environmental conscious, and the desire to reduce construction costs. Consequently, reuse and recycling of concrete have received a great deal of attention, from the late 1980s or early 1990s (Xu et al., 2017; Xuan et al., 2018). Waste concrete was initially reused in the new concrete based on OPC (Verian et al., 2018; Xu et al., 2018), and then has strived for the application in geopolymer composites, with the booming development in geopolymer technology (Tang et al., 2020).

Most efforts making use of waste concrete in geopolymer composites are through using it as recycled aggregates, including coarse and fine aggregates. In literature, the attention has been mostly focused on the influences of various factors (e.g., chemical activators, raw materials, curing regimes, and replacement ratio) on the performance of geopolymer composites containing recycled concrete aggregates, with regards to the mechanical, durability, and microstructural properties. Table 3 presents the summary of the existing studies that utilized waste concrete as aggregate in geopolymer mortar and concrete. Broadly, the incorporation of recycled concrete aggregate degrades the performance of geopolymer composites, be it the mechanical or durability properties. Taking the compressive strength as an example, Fig. 11 demonstrates the declining compressive strength of geopolymer composites with the increase of recycled concrete aggregate replacement ratio. Nevertheless, as shown in Table 3, the geopolymer composites containing recycled concrete aggregate could still fit a wide range of strength requirements through amending characteristics of the source materials or alkaline activating solution, optimizing the ingredient portion, and choosing the suitable curing method (Koushkbaghi et al., 2019).

On the other hand, some advantages of geopolymer composites incorporating recycled concrete aggregates have been reported. Because of the different matrix formation process, the geopolymer paste is composed of a more homogeneous and denser substance compared to OPC paste (Shi et al., 2012). Moreover, the geopolymer matrix could fill the pre-existing incomplete interphase within the recycled concrete aggregate (Khedmati et al., 2018). This might result in that the geopolymer matrix was tightly bonded to recycled concrete aggregate, and thus, no obvious interfacial transition zone (ITZ) could be identified between the recycled concrete aggregate and new geopolymer binders (Liu et al., 2016). Also, the lower autogenous and drying shrinkage could be detected in the geopolymer mortars after the inclusion of recycled concrete aggregates, which was related to the function of recycled concrete aggregate as an internal curing agent (Lee et al., 2018). Recently, Sedaghatdoost et al. (2019) reported that utilizing recycled concrete aggregates boosted the resistance of geopolymer composites to elevated temperatures, up to 800 °C.

Previous studies have also suggested some valid approaches that could overcome the adverse effects due to the recycled concrete aggregate replacement, and subsequently, improve the performance of geopolymer composites containing recycled concrete aggregate

(Nuaklong et al., 2018b). Among them, the incorporation of calcium-carrying materials, such as slag and OPC, was the most effective and practical one (Hu et al., 2019; Tang et al., 2019a; Xie et al., 2019a). For instance, Xie et al. (2018) observed the significant increases in compressive strength, elastic modulus, and energy absorption, with the increase in the slag content. This was also supported by the results of Hu et al. (2019) and Xie et al. (2019a), that the improvement in the microstructural properties was identified after the incorporation of calcium-carrying materials.

Few researchers (Ahmari et al., 2012; Gong et al., 2014; Komnitsas et al., 2015; Vásquez et al., 2016) have investigated the recycling of waste concrete for geopolymer precursors. The average, maximum, and minimum values for the chemical composition of the waste concrete powder (WCP) from selected studies are provided in Fig. 12(a). In addition, the mineralogy of WCP is illustrated in Fig. 12(b). It has been suggested that there is a low content of amorphous aluminosilicate existed (Ahmari et al., 2012). Therefore, in the existing practices, WCP was usually blended with other conventional geopolymer precursors, and then was activated by alkaline solution. The influences of the content of WCP, the composition and concentration of the alkaline solution, and the type of curing were evaluated. It has been concluded that the appropriate design was important to achieve the suitable properties of the final product. For instance, in the test conducted by Ahmari et al. (2012), the inclusion of WCP below a certain content helped improve the compressive strength of geopolymer binder based on CFA, while the further increase led to the strength degradation. Furthermore, Abdel-Gawwad et al. (2018) developed a one-part geopolymer by activation of WCP blended with a certain amount of sodium hydroxide under elevated temperature. The resulted geopolymer product could yield a hardened matrix with compressive strength up to 79 MPa at 28 days.

3.2. Waste clay brick

Clay bricks are respected to be the second most common construction material after concrete. The waste clay brick (WCB) originates not only from demolition activities, but also from the rejected bricks during the manufacturing, transporting, and construction processes. Clay bricks are produced by mixing ground clay with water, forming the clay into the desired shape, and then drying and firing. Fig. 13(a) shows the average, maximum, and minimum values for the chemical composition of WCB collected from the selected studies. In particular, clay brick contains high levels of SiO₂ and Al₂O₃ and therefore is considered to have great potential as a geopolymer precursor.

Table 4 summarizes the previous research studies assessing the feasibility of WCB as the precursor of geopolymer composites. It is concluded that WCB could provide a valid alternative to the precursor material for geopolymer composites (Peyne et al., 2017). Also, in order to achieve better performance, a number of researchers optimized the formation of WCB-based geopolymers by varying the alkaline solution parameters such as the alkaline type, silica modulus, and alkaline concentration, as well as, the curing condition and water/binder ratio (Fořt et al., 2018; Keppert et al., 2018; Komnitsas et al., 2015; Reig et al., 2013a). For instance, Tuyan et al. (2018) investigated the effect of alkali concentration (4–10 %), silica modulus (0–2.2), curing temperature (50–90 °C), and curing duration (1–7 days) on the consistency and strength of WCB-based geopolymer mortar. Test results demonstrated that the optimum activator composition had an alkali concentration of 10 % and a silica modulus of 1.6, and the maximum compressive strength was obtained upon curing at 90 °C for 5 days.

Nevertheless, it should be noted that in order to attain sufficient mechanical strengths, the WCB-based geopolymer composites were mostly synthesized under the curing conditions with high temperatures (usually above 60 °C) and a long period. This is mainly attributed to the high content of crystalline mineral and the lower concentration of amorphous matter in WCB (as shown in Fig. 13(b)), resulting in a

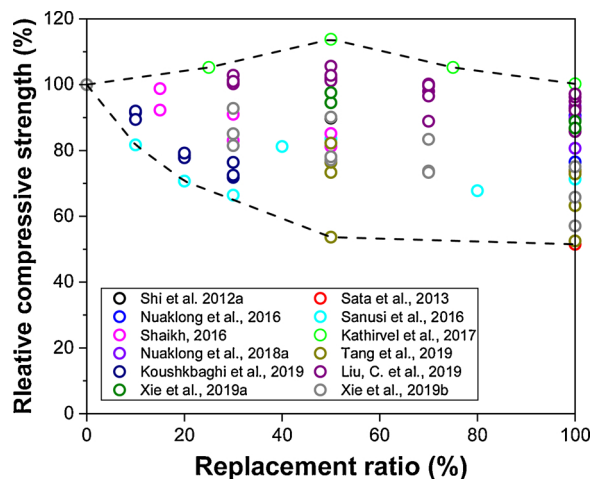


Fig. 11. Relationship between the replacement ratio of waste concrete and relative compressive strength.

relatively low geopolymerization reaction with low/no strength development at an early age (Keppert et al., 2018; Tuyan et al., 2018). This kind of curing condition apparently increases the cost of production and energy demand, and also hindering its application in cast-in-suit construction (Hwang et al., 2019b). For this reason, it is preferable to use WCB in a blend with other reactive material, such as metakaolin, fly ash, and OPC, to achieve an effective geopolymerization process without high temperature. In the study of Hwang et al. (2019b), high-strength geopolymer pastes using a high volume of WCB as source materials were developed under ambient temperature curing. In these mixtures, WCB composed 60 % of the total mass of the starting materials, while CFA and GGBFS with different portions composed the remaining 40 %. The resulted samples could achieve the compressive strength ranging from 36 to 70 MPa, whereas the control mixture based on sole WCB did not set even after 24 h of casting. Robayo et al. (2016) also indicated that the inclusion of 20 % OPC could yield WCB-based geopolymer pastes with the compressive strength of 102.6 MPa after 28-day ambient curing, which was twice the strength obtained in the mixture without OPC.

There also exist other studies concentrating on the use of crushed clay brick as coarse or fine aggregates in geopolymer products (Reig et al., 2017; Sata et al., 2013; Wongsa et al., 2018b). As brick aggregate is comparatively weaker and more porous than virgin aggregate, the significant reduction in the mechanical strength has been observed when the recycled brick was used as aggregate substitute in geopolymer concrete and mortar (Reig et al., 2017; Sata et al., 2013; Wongsa et al., 2018b). However, by harnessing the low density feature of clay brick, Wongsa et al. (2018b) employed clay brick aggregate to produce lightweight geopolymer concrete, with the densities ranging from 1685 kg/m³ to 1749 kg/m³. The test results also demonstrated that the use of crushed clay brick as coarse aggregate could equip geopolymer concrete with excellent thermal insulation, and thermal resistance under the temperatures of 400–800 °C. In another study, pervious geopolymer concrete was successfully developed using crush clay brick aggregate, which contained continuous voids and possessed high water permeability (Sata et al., 2013).

3.3. Ceramic waste

Ceramic materials and products are often applied in building decoration projects, such as floor-wall tiles, garden ceramic, terracotta products, and sanitary ceramic. The production of ceramics is similar to that of clay brick: normally starts from raw material, mixing, molding, burning, polishing, and glazing. While ceramic materials are usually fired at a higher temperature than bricks so that the silica re-crystallizes

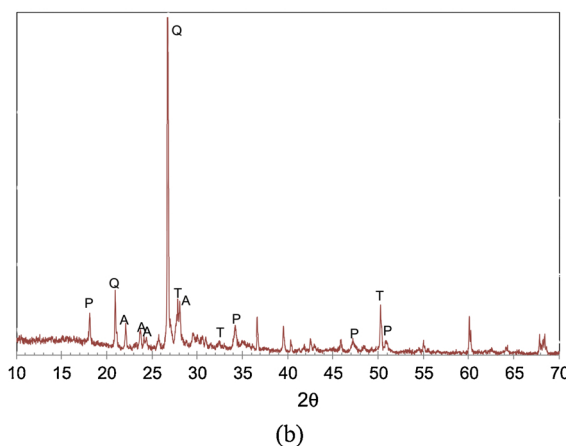
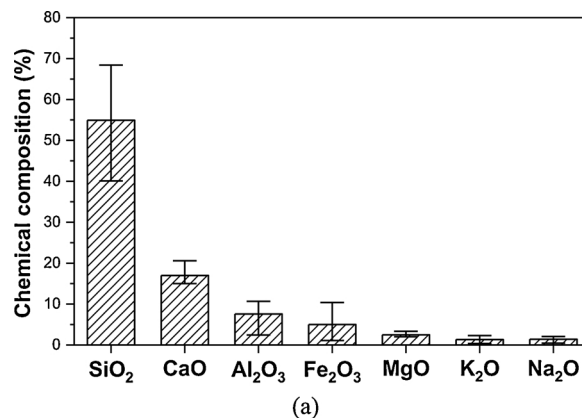


Fig. 12. Chemical composition and mineralogy of WCP: (a) Chemical composition of WCP from the selected studies. Data from (Abdel-Gawwad et al., 2018; Ahmari et al., 2012; Vázquez et al., 2016); (b) XRD pattern of WCP (A: anorthite, M: mullite, P: portlandite, Q: quartz, T: 1.1-nmtobermorite) (Ahmari et al., 2012).

to form a glassy material, having greater density, strength, hardness, resistance to chemicals and frost, and greater dimensional stability. Fig. 14 presents the average, maximum, and minimum values for the chemical composition of ceramic waste powder (CWP) from the selected studies, as well as the XRD pattern. The chemical composition of ceramic, along with highly amorphous aluminosilicate, makes it possible to manufacture geopolymer composites. Therefore, utilizing CWP as the precursor materials in geopolymer formulation has gained great academic interest.

As shown in Table 5, it summarizes the recent studies on CWP-based geopolymer composites. Among these, part of the studies investigated the properties of geopolymer composites completely based on CWP. Reig et al. (2013b) first formulated geopolymer mortars based on CWP, and also analyzed the impact of the alkali activator concentration on the mechanical strength and microstructure of the mortars formed. It was manifested that at a constant water-to-binder ratio, increasing the alkali concentration from 6.0% to 9.0% increased the compressive strength of CWP-based geopolymer mortar from 25 MPa to 29 MPa. Afterwards, further research has been done aiming to understand the geopolymerization process of CWP, and to enrich the technical data on the effect of particle size, curing condition, and alkaline solution properties on the performance of final products (Amin et al., 2017; Komnitsas et al., 2015; Shoaie et al., 2019; Usha et al., 2016). In short, CWP exhibits high geopolymerization potential, which is even better compared with waste bricks and concrete (Komnitsas et al., 2015). Moreover, by optimizing the initial reacting system and the alkaline activating solution, a well geopolymerization process and better

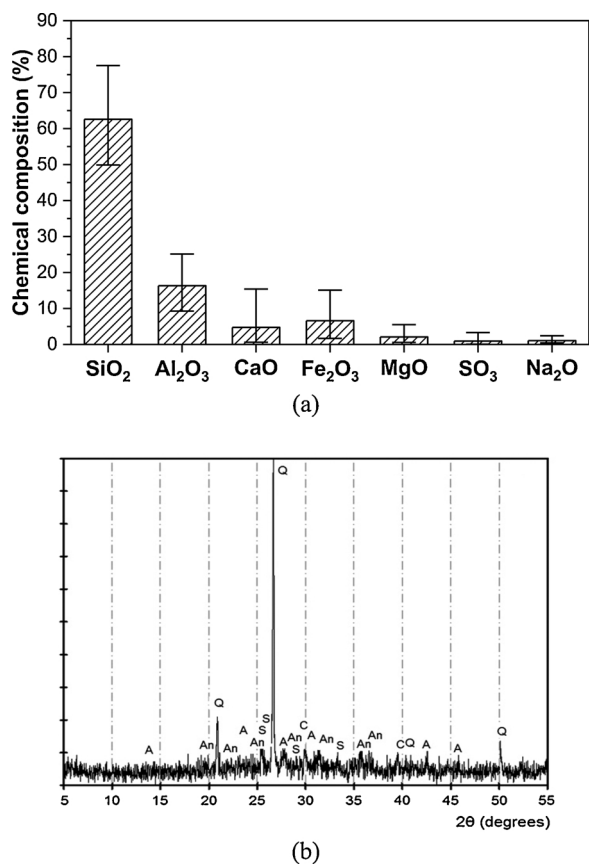


Fig. 13. Chemical composition and mineralogy of WCB: (a) Chemical composition of WCB from the selected studies. Data from Fořt et al. (2018); Hwang et al. (2019a); Keppert et al. (2018); Komnitsas et al. (2015); Ouda (2019); Rakhimova and Rakhimov (2015); Reig et al. (2016); Robayo et al. (2016); Rovnanřk et al. (2018); Sedira et al. (2018); Silva et al. (2019a); Tuyan et al. (2018); Wongsā et al. (2018b); Zawrah et al. (2016). (b) XRD pattern of WCB (Q: Quartz; A: Albite; An: Anortite; S: Sanidine ; C: Calcite) (Reig et al., 2013a).

performance of final products could be obtained.

Furthermore, a number of studies have evaluated the performance of geopolymer composites based on the combination of CWP and other aluminosilicate precursors. The group of Huseien conducted a series of investigations on the workability, strength, and durability properties of multi-blend geopolymer pastes and mortars containing CWP (Huseien et al., 2018b, a; Huseien et al., 2019b). Specifically, the majority of the starting material was CWP, and the remaining consisted of CFA and GGBFS. The findings suggested that high volume CWP could produce geopolymer composites with compressive strength over 70 MPa. Also, the developed geopolymer composites exhibited enhanced resistance to elevated temperature with the increase of CWP content, which also has been verified by Sun et al. (2013). Similarly, researchers blended CWP with metakaolin and even waste glass powder to synthesize geopolymer composites, and the resulted products also exhibited satisfactory performance (Huseien et al., 2018a; Ramos et al., 2018).

In addition to utilizing ceramic waste as the precursor materials, the other possible application of ceramic waste is using as aggregate replacement in geopolymer mortar and concrete (Abdollahnejad et al., 2019; Hwang et al., 2019b; Reig et al., 2017). Particularly, in the studies by Abdollahnejad et al. (2019) and Reig et al. (2017), the ceramic waste was used as both a precursor and recycled aggregate. It has been observed that after immersion in the activating solution, the original rounded pores of ceramic waste aggregates could not be distinguished clearly, and crystalline particles accumulated into the pore network (as seen in Fig. 15). These changes denoted the dissolution of the ceramic waste aggregates by the activating solution, and thus created a good ITZ

Table 4
Recent research of the geopolymer composites made from waste clay brick.

Composites	Precursor ¹	WCB content (wt.%)	Activator	Curing condition		Compressive strength (MPa)	Reference
				Temperature	Duration		
Mortar	WCB + GGBFS	100	NaOH + Na ₂ SiO ₃	65 °C	3 or 7 days	7.1–50.0 (7 days)	Reig et al. (2013a)
	WCB	20, 40, 60, 80, 100	NaOH + Na ₂ SiO ₃ ; NaOH	95 °C, RT	12 hrs	26–112.3 (28 days)	Rakhimova and Rakhimov (2015)
	WCB	100	NaOH + Na ₂ SiO ₃ ; SH	50, 60, 70, 80, 90, 100 °C, RT	1, 3, or 7 days	4.0–36.2 (7 days)	Tuyan et al. (2018)
Paste	WCB + GGBFS	50, 60, 70, 80, 90, 100	NaOH + Na ₂ SiO ₃ ; NaOH	RT	—	23.1–91.3 (28 days)	Hwang et al. (2019b)
	WCB	100	NaOH + Na ₂ SiO ₃	60, 80, or 90 °C	7 days	4.7–49.5 (7 days)	Komnitsas et al. (2015)
	WCB + CAC	50, 60, 70, 80, 90, 100	NaOH + Na ₂ SiO ₃	65 °C, RT	3 or 7 days	4.1–93.7 (7 days)	Reig et al. (2016)
	WCB + OPC	80, 90, 95, 100	NaOH + Na ₂ SiO ₃ ; NaOH	70 °C, RT	1 or 2 days	7.5–102.6 (28 days)	Robayo et al. (2016)
	WCB + GGBFS	20, 40, 60, 80, 100	NaOH + Na ₂ SiO ₃	RT	—	11.7–79.2 (28 days)	Zawrah et al. (2016)
	WCB + OPC	70, 80, 90, 100	Na ₂ SiO ₃ ; NaOH; Na ₂ SO ₃	RT	—	10.2–102.7 (28 days)	Robayo et al. (2016)
	WCB	100	NaOH + Na ₂ SiO ₃	RT	—	10.3–41.9 (28 days)	Fořt et al. (2018)
	WCB	100	NaOH + Na ₂ SiO ₃	RT	—	27.5–38.8 (28 days)	Keppert et al. (2018)
	WCB + MK	25, 50, 75, 100	NaOH + Na ₂ SiO ₃	40 °C	20 hrs	6.6–26.5 (14 days)	Rovnanřk et al. (2018)
	WCB + TMWM	10, 20, 30, 40, 50	NaOH + Na ₂ SiO ₃	RT	—	25–59 (28 days)	Sedira et al. (2018)
	WCB + GGBFS + CFA	60, 100	NaOH + Na ₂ SiO ₃	RT	—	38.2–68.2 (28 days)	Hwang et al. (2019a)
WCB + DCP	70, 80, 85, 90, 95, 100	NaOH	80 °C	1 day	3.0–51.4 (28 days)	Ouda (2019)	
WCB + NP	100	NaOH + Na ₂ SiO ₃	65, 80, 95 °C	1, 3, or 7 days	0.7–37.0 (28 days)	Silva et al. (2019a)	

Note: 1. CAC, TMWM, DCP, and NP denote calcium aluminate cement, tungsten mining waste mud, dolomite-concrete powder, and natural pozzolana, respectively.

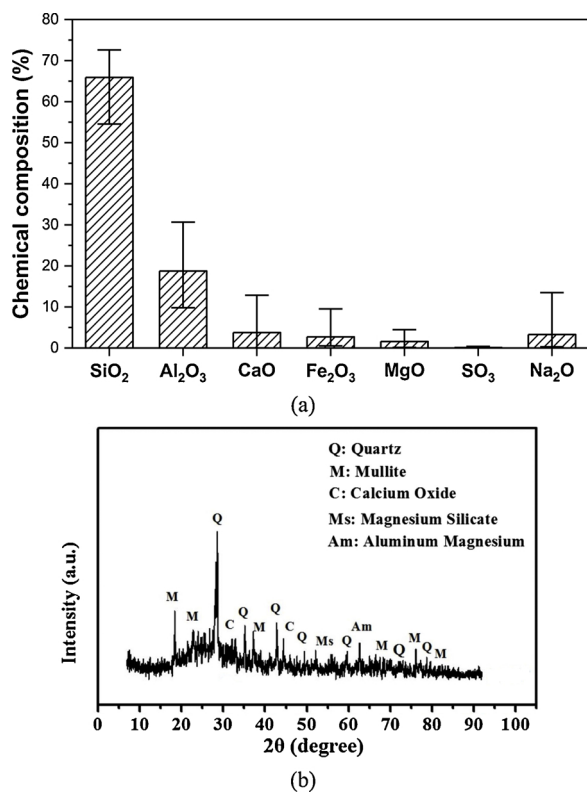


Fig. 14. Chemical composition and mineralogy of CWP: (a) Chemical composition of CWP from the selected studies. Data from [Abdollahnejad et al. \(2019\)](#); [Aly et al. \(2018\)](#); [Amin et al. \(2017\)](#); [Huseien et al. \(2019b\)](#); [Hwang et al. \(2019a\)](#); [Komnitsas et al. \(2015\)](#); [Ramos et al. \(2018\)](#); [Reig et al. \(2013b\)](#); [Shoaei et al. \(2019\)](#); [Sun et al. \(2013\)](#); [Usha et al. \(2016\)](#); (b) XRD pattern of CWP ([Huseien et al., 2020](#)).

([Hwang et al., 2019b](#)). As a result, the strength of geopolymer mortar was improved by adding ceramic waste aggregates, up to 43 MPa under the optimum percentage of 50 wt.% ([Abdollahnejad et al., 2019](#)).

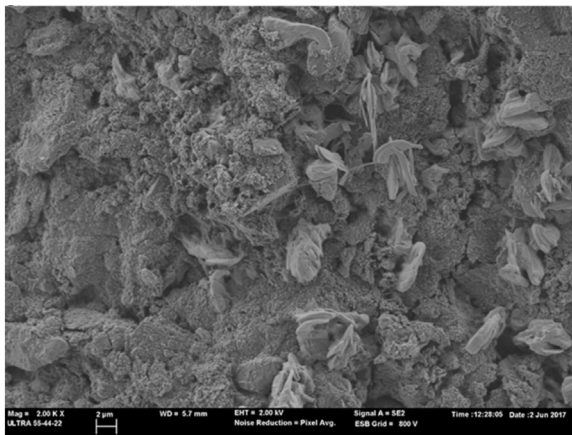
3.4. Waste asphalt pavement

Waste asphalt pavement (WAP) is generated when existing asphalt pavements are removed for reconstruction, resurfacing, or gaining access to buried utilities. When properly crushed and screened, WAP consists of high-quality and well-graded aggregates coated by aged asphalt. The recycling of WAP rates relatively high (such as 47 % in Europe and 84 % in the US), mainly through hot and warm mix asphalt processes. However, a large quantity of WAP materials remains unutilized yet ([Zaumanis et al., 2014](#)). Recent investigations have shown that the problem of WAP can be solved by using WAP as base and subbase aggregate materials. Several researchers have successfully adopted geopolymers to stabilized WAP material as pavement base or subbase applications.

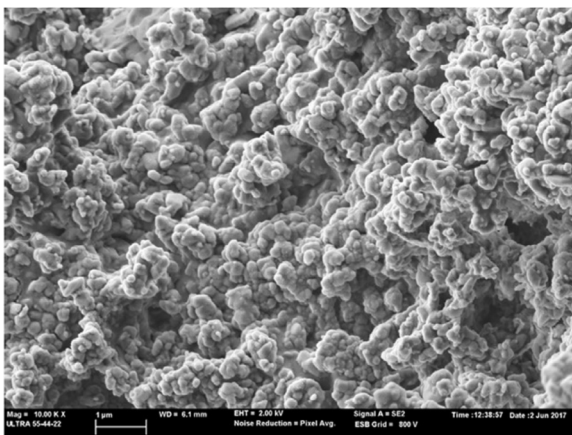
[Mohammadinia et al. \(2016a, 2016b\)](#) have demonstrated that the CFA and/or slag-based geopolymer stabilization considerably enhanced the mechanical properties (e.g., unconfined compressive strength and elastic modulus) of WAP. It was additionally proved that the mechanical strength of stabilized WAP materials increased with the increase of geopolymer binder content. This result was also in agreement with that obtained by [Saride et al. \(2016\)](#), who investigated the performance of specimens prepared at various proportions of WAP and natural aggregate, stabilized by CFA-based geopolymer. In addition, it has been found that the amount of exposed aggregate surface of WAP particles played a major role in the strength characteristics ([Saride et al., 2016](#)). It is attributed to that the WAP particles are coated with the amorphous asphalt layer, which will reduce the strength of the cementitious bond created by geopolymer binders. Besides that, Hoy's research team evaluated the strength development and microstructural of geopolymer-stabilized WAP ([Hoy et al., 2016a, 2018](#)). In the mixes, CFA or

Table 5
Recent research of the geopolymer composites made from ceramic waste powder.

Composite type	Precursor	WCT content (wt.%)	Activator	Curing condition		Compressive strength (MPa)	Reference
				Temperature	Duration		
Mortar	CWP	100	NaOH + Na ₂ SiO ₃	60, 75, 90, 105 °C	24 hrs	22.2–27.9 (28 days)	Shoaei et al. (2019)
	CWP + GGBFS + CFA	50	NaOH + Na ₂ SiO ₃	RT	—	45.9–66.2 (28 days)	Huseien et al. (2019b)
	CWP + GGBFS + CFA	50, 60, 70	NaOH + Na ₂ SiO ₃	RT	—	22.2–70.1 (28 days)	Huseien et al. (2018b), a
	CWP + GGBFS	10, 20, 30	NaOH + Na ₂ SiO ₃	60 °C, RT	3 hrs	10.3–17.9 (28 days)	Abdollahnejad et al. (2019)
	CWP + GP + GGBFS + CFA	15	NaOH + Na ₂ SiO ₃	RT	—	30.1–54.0 (28 days)	Huseien et al. (2018a)
	CWP + GGBFS	60, 80, 90, 100	NaOH, KOH	60 °C, RT	24 hrs	6.2–32.8 (7 days)	Aly et al. (2018)
	CWP	100	NaOH + Na ₂ SiO ₃	65 °C	3 days	9.4–32.3 (3 days)	Reig et al. (2017)
	CWP	100	NaOH + Na ₂ SiO ₃	35, 45, 55, 65, 75 °C	24 hrs	7.1–26.5 (28 days)	Usha et al. (2016)
	CWP	100	NaOH + Na ₂ SiO ₃	65 °C	7 days	25.6–29.5 (7 days)	Reig et al. (2013b)
	CWP	100	NaOH + Na ₂ SiO ₃	RT	—	34.6–58.0 (28 days)	Hwang et al. (2019a)
Paste	CWP + GGBFS + CFA	60, 100	NaOH + Na ₂ SiO ₃	RT	—	34.6–58.0 (28 days)	Hwang et al. (2019a)
	CWP + MK	15, 30, 45	NaOH + Na ₂ SiO ₃	RT	—	20.5–71.6 (28 days)	Ramos et al. (2018)
	CWP	100	NaOH + Ca(OH) ₂	RT	—	2.3–8.0 (28 days)	Amin et al. (2017)
	CWP	100	NaOH + Na ₂ SiO ₃	60, 80, 90 °C	7 days	1.5–57.8 (7 days)	Komnitsas et al. (2015)
	CWP	100	NaOH + Na ₂ SiO ₃ ; KOH + Na ₂ SiO ₃ ; NaOH + KOH; NaOH	60 °C	27 days	30.5–71.2 (28 days)	Sun et al. (2013)



(a) General view



(b) Solid-phase magnification

Fig. 15. Microstructures of the ceramic waste aggregates after immersion in the alkali-activating solution (Reig et al., 2017).

slag was activated with a combination of sodium hydroxide solution and sodium silicate solution and then was used to stabilize the WAP. The test results confirmed that these products met the related specification, as shown in Fig. 16, and therefore could be used as a base course material in road work. Fig. 16 also reveals that the increased NaOH content contributes to the superior performance, which is due to the more steady three-dimensional formation of the aluminosilicate geopolymer structure (Hoy et al., 2017). Furthermore, the existing studies (Avirneni et al., 2016; Hoy et al., 2016b, 2017) on permanency in terms of wet-dry cycles and toxic leaching showed that geopolymer stabilized WAP also performed satisfactorily.

3.5. Other wastes

3.5.1. Asbestos

Asbestos-containing materials have been used for insulation in buildings and in various products such as roofing materials, water supply lines, and wall cladding, owing to the excellent tensile strength, poor heat conduction, and high resistance to chemical attack. However, asbestos is considered to be extremely carcinogenic, and the mining and use of asbestos have been banned in most countries since the beginning of the 80 s. Nevertheless, challenges remain in the disposal of asbestos-contaminated waste materials, presenting as an issue of global concern.

Physical, thermal, chemical, and biological treatments have been proposed to transform asbestos-contaminated materials into nonhazardous materials (Spasiano and Pirozzi, 2017). But for these end-products, a suitable and attractive recycling solution is being sought. Gualtieri et al. (2012) successfully employed the product of asbestos-cement after thermal treatment for the formulation of geopolymers. The treated asbestos-cement contained Al-, Ca-, Mg-rich silicates (SiO_2 : 30.8 %, Al_2O_3 : 5.4 %, CaO: 48.5 %, MgO: 7.5 %). The test results indicated that the addition treated asbestos-cement could promote the geopolymerization reaction, and meantime allowed to increase the physical and mechanical characteristics of the geopolymers, demonstrating the potential of recycling treated asbestos waste in geopolymer composites.

3.5.2. Mineral wool

Mineral wool is the fibrous material formed by spinning or drawing molten mineral or rock materials. The applications of mineral wool mainly include thermal insulation (such as structural insulation and pipe insulation), and soundproofing. In literature, the study on the reuse of mineral wool waste remains low. Yliniemi et al. (2019) investigated the suitability of mineral wool waste for geopolymer precursor material. In the study, mineral wool waste (stone wool and glass wool) collected from building demolition and construction sites was milled into powder and then used as a geopolymer precursor. A range of 25–45 MPa was reported for the compressive strength of the resulted geopolymer pastes at 28 days. Furthermore, excellent durability under the aggressive freeze-thaw was observed for the prepared geopolymer pastes. This study provided valuable information for promoting the utilization of mineral wool waste as a geopolymer precursor.

4. Discussion

Table 6 presents the general view of the characteristics of solid waste studied, as well as their usages and respective performance of the resulted geopolymer composites. It could be observed that recycling these solid waste materials in geopolymer composites shares some commons, and therefore the experiences achieved can be shared with each other. Overall, both the municipal and construction solid waste materials can be potentially recycled, as the forms of precursor, aggregate, additive, reinforcement fiber, and filling materials, to fabricate the sustainable green concept geopolymer composites. Although the utilization of solid waste materials provides geopolymer composites with value-added significances, precaution must be taken to the certain detrimental effects caused by the use of waste, and this can be achieved by carefully selecting the inclusion content. Also, if considering the use of municipal and construction solid waste for the mass production of geopolymer composites, there is a need to assess the consistency and availability of materials supply in the waste streams as well as the distance to the geopolymer product manufactures.

Moreover, suitable treatments, such as the water-wash treatment, proper incineration course, and mechanical grinding, are well recognized to boost the behavior of these solid waste-containing geopolymer products. Another way to say, the usage of waste materials in geopolymer composites could be greatly maximized without compromise in the performance of final geopolymer products. However, there are some barriers to be overcome. Mostly, high costs and energy consumption demanded, especially by physical and thermal treatments, will drive down the environmental friendliness of the products from a global point of view (Gualtieri et al., 2012). Besides, as for the processes of chemical treatment, in addition to a large number of reagents necessary, the fate of the post-treatment reagents remains an issue of considerable concern (Spasiano and Pirozzi, 2017). As a consequence, it

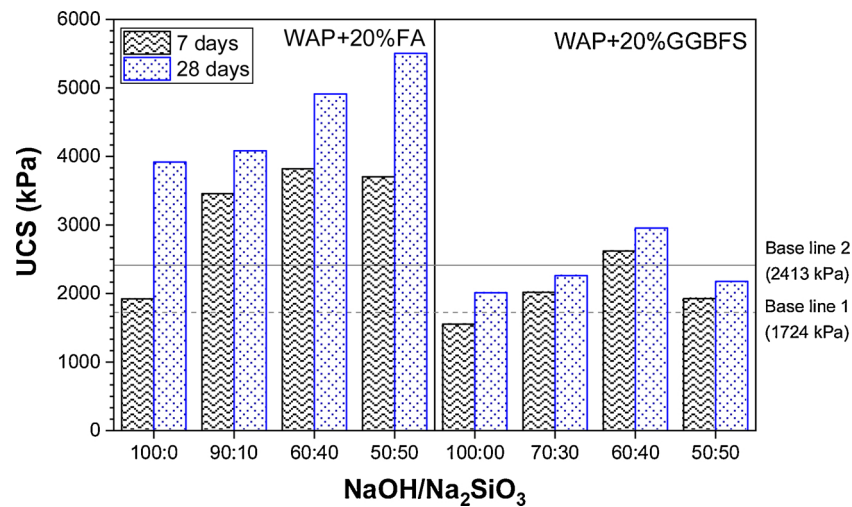


Fig. 16. Unconfined compressive strength (UCS) of WAO-CFA blends and WAO-GGBFS blends at 7 and 28 days (Hoy et al., 2016a, 2018).

is greatly advised to compile and examine the impacts associated with energy and material inputs and environmental releases for each treatment scenario. For this purpose, life cycle assessment is an effective tool, which can support decision-makers on waste treatment options and provide information on the attendant risks (Chen et al., 2019; Khandelwal et al., 2019; Kurda et al., 2018). Furthermore, advanced new technical methods are in high demand to overcome the defects of conventional treatment methods. For instance, Shi et al. (2016) recommended the carbonation treatment for recycled concrete aggregates, which is not only an efficient way for enhancing the properties of recycled concrete aggregate but also an environmental friendly approach.

Fig. 17 compares the main chemical composition (i.e., calcium, silica, and alumina oxides) of the different solid waste materials. Apparently, a wide variation in the main chemical composition occurs due to the differences in their types and sources. Besides, the contents of other chemical compounds also vary according to the diverse sources of solid waste, which can be seen from the previous sections. Furthermore, different solid waste materials also have various physical properties and mineralogical composites (Provis, 2013; Reddy et al., 2016). All these diversities contribute to the disparate behavior of synthesized geopolymer composites (Provis et al., 2015). This, therefore, highlights the significance of the elucidation and modeling for geopolymerization reaction kinetics and mechanisms based on different source materials. It is because that high understanding could serve as a guideline for the geopolymer researchers in identifying the crucial parameters during the design and fabrication stage, and also linking between the performance of resulting geopolymer composites and the properties of source materials and formulation conditions. Thus, the true value of solid waste materials can be realized and unlocked. Additionally, since the solid waste materials are often mineralogically heterogeneous and complex, and often span a broad range of particle shapes and sizes, it also emphasizes the importance of the advanced characterization techniques for precursor materials, which is required to smooth the above step (Provis et al., 2015).

To promote the recycling of solid waste materials in geopolymer composites or other recycling approaches, the necessity of effective solid waste management plans and strategies is also evident. Further, waste sorting is the key step in waste management to ensure a higher rate of recycling (Ajayi et al., 2015). It is because that the municipal and construction solid waste often contains a wide variety of materials,

and mixed and contaminated waste is not suitable for recycling, while sorting could separate the waste into different groups in line with its components. Only through waste sorting, more valuable components can be picked up for recycling. Against this scenario, more effective separation and sorting techniques, as well as the corresponding machinery, should be implemented to the waste stream, regardless of on-site or off-site operations (Gundupalli et al., 2017). In addition, the increasing awareness and participation of the public and relevant stakeholders are the critical components in the management program of municipal and construction waste. Finally, yet importantly, intervention and support from the government should be enhanced. Such support can include providing tax refunds for contractors who recycle waste materials, establishing recycling markets, setting up incentive-based market support, and granting no-interest loans for small companies to begin and expand their recycling projects (Huang et al., 2018a; Sun et al., 2018).

5. Conclusion

Accumulation of unmanaged municipal and construction solid waste has been an increasing environmental concern. Recycling of such solid waste into sustainable and energy-efficient construction materials is a viable approach to relieve the stress of pollution and meantime to conserve virgin resources for the next generation. This study has critically reviewed the potential applications of diverse municipal and construction solid waste as substitute materials in manufacturing sustainable geopolymer composites, specifically, in the form of partial or even fully substitution of precursors or aggregates, reinforcement fiber, or additives. Conclusively, even though the incorporation of the studied waste materials into geopolymer composites adversely affects their few attributes, such as strength, workability, and durability, satisfactory performance can be still maintained through controlling its quantity percentage in accordance with the outcomes of the current work. Additionally, these waste materials could be recycled in geopolymer composites with a high rate if proper treatment is carried out or suitable proportion design is adopted, attributing to the improved mechanical and durable performance of the final products. Finally, there are still a number of areas that require additional attention, especially from the scientific and technological perspectives in the field of geopolymer, as well as, the advance in the solid waste management plans and strategies. In short, this study shows an economical and sustainable

Table 6
General view of waste materials characteristic, usages and respective performance of resulted geopolymer composites.

Waste materials	Characteristics	Solid waste usage	Inclusion content	Performance of resulted geopolymer composites
Municipal solid waste				
Municipal solid waste incinerator bottom ash	Contains metallic aluminum, contains heavy metals, porous structure	Precursor	Up to 100 % can be used (after the alkaline pre-treatment)	<ul style="list-style-type: none"> - Decreased compressive strength - Highly porous structure - Immobilized hazardous elements - Highly porous structure - Decreased compressive strength - Decreased compressive strength - Controlled hazardous elements leaching
Municipal solid waste incinerator fly ash	High content of heavy metal, chlorides and sulfates, low reactivity	Additive Fine aggregate Precursor	Up to 50 % can be used A maximum of 50 vol.% is recommended Only 20 wt.% or lower percentage is recommended, or 100 % can be used after water-wash pre-treatment	<ul style="list-style-type: none"> - Decreased workability - Decreased drying shrinkage - Decreased workability - Increased setting time - Increased compressive strength - Increased drying shrinkage - Decreased density - Decreased mechanical properties (e.g., compressive, splitting tensile and flexural strength, elastic modulus) - Increased thermal and sound insulation - Increased ductility - Increased impact resistance and damping property - Decreased surface abrasion resistance - Increased tension strength (only as fiber reinforcement) - Decreased compressive strength - Increased flexural strength - Increased toughness - More ductile behavior - Suitable mechanical properties for subgrade material (e.g., compressive strength and stiffness) - Increased electromagnetic interference shielding properties - Decreased compressive strength
Waste paper sludge	Contains organic matter and cellulose fiber	Precursor	A maximum of 10 wt.% can be used	
Waste paper sludge ash	High reactivity, high calcium content	Precursor	Up to 100 % can be used	
Rubber waste	Low density, hydrophobic nature, low stiffness, high deformability, good sound and thermal insulation, high toughness and impact resistance	Aggregate Fiber reinforcement	A maximum of 10 wt.% or 20 vol.% is recommended Up to 30 wt.% can be used	
Plastic waste	Low density, low stiffness, high deformability, good sound and thermal insulation, not easily biodegradable	Fine aggregate Fiber reinforcement	A maximum of 20 vol.% is recommended A maximum of 2 wt.% can be used	
Tire steel and textile fiber	Tire steel fiber: High tensile strength, high density, potential corrosion Tire textile fiber: High tensile strength, low density	Fiber reinforcement	Tire steel fiber: a maximum of 2 vol.% can be used Tire textile fiber: a maximum of 20 vol.% is recommended	
Spent coffee grounds	Highly organic material, Low shear strength, high compressibility,	Filling material	A maximum of 70 wt.% is recommended	
Waste cork	High carbon content (after thermal treatment)	Additive	A maximum of 3.75 wt.% can be used	
Construction solid waste				
Waste concrete	Poor strength, high porosity, relatively low reactivity	Precursor	Up to 100 % can be used	As aggregate usage:
Waste clay brick	Low density, poor strength, high porosity, good fire resistance, relatively low reactivity	Aggregate		<ul style="list-style-type: none"> - Decreased density and increased porosity - Decreased mechanical properties (e.g., compressive, splitting tensile and flexural strength, elastic modulus) - Decreased durability properties (e.g. chemical attack, abrasion resistance) - Increased thermal insulation and thermal resistance (waste clay brick and ceramic waste) - As precursor usage: - Decreased mechanical properties (e.g. compressive, splitting tensile and flexural strength) - Increased thermal resistance (ceramic waste) - Suitable mechanical properties for base/subbase applications (e.g., compressive strength and stiffness) - Decreased cementitious bond - Decreased porosity - Increased flexural strength - Increased freeze-thaw durability
Ceramic waste	Low density, poor strength, high porosity, good fire resistance, high reactivity			
Waste asphalt pavement	High porosity, contain heavy metal, aged asphalt coating	Filling material	A maximum of 80 wt.% is recommended	
Asbestos-containing cement	Chemically comparable to an Mg-rich clinker, high reactivity (after thermal treatment)	Additive	A maximum of 2.5 wt.% is recommended	
Mineral wool	High reactivity	Precursor	Up to 100 % can be used	

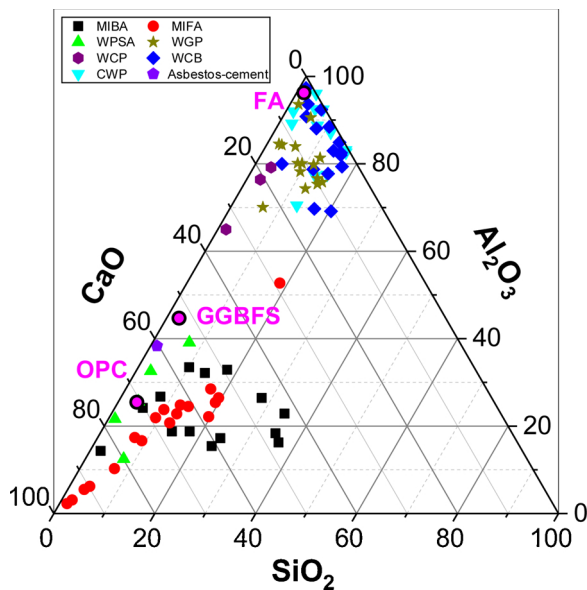


Fig. 17. The ternary diagram of silica, alumina, and calcium oxide content in municipal and construction solid waste. Data from the results of Figs. 2,4,5,9,12,14, and 15, and the study of Gualtieri et al. (2012) for asbestos-cement.

alternative for the disposal of municipal and construction solid waste by recycling it into manufacturing sustainable construction materials.

Declaration of Competing Interest

The authors whose names are listed immediately below certify that they have NO affiliations with or involvement in any organization or entity with any financial interest (such as honoraria; educational grants; participation in speakers' bureaus; membership, employment, consultancies, stock ownership, or other equity interest; and expert testimony or patent-licensing arrangements), or non-financial interest (such as personal or professional relationships, affiliations, knowledge or beliefs) in the subject matter or materials discussed in this manuscript.

Acknowledgements

All the authors appreciate the financial supports from the Australian Research Council (ARC) (DE150101751), University of Technology Sydney Research Academic Program at Tech Lab (UTS RAP), University of Technology Sydney Tech Lab Blue Sky Research Scheme, and the Systematic Projects of Guangxi Key Laboratory of Disaster Prevention and Structural Safety (Guangxi University), China (2019ZDX004) and State Key Laboratory of Subtropical Building Science (South China University of Technology), China (2019ZA06).

References

Abdel-Gawwad, H.A., Heikal, E., El-Didamony, H., Hashim, F.S., Mohammed, A.H., 2018. Recycling of concrete waste to produce ready-mix alkali activated cement. *Ceram. Int.* 44 (6), 7300–7304.

Abdollahnejad, Z., Luukkonen, T., Mastali, M., Kinnunen, P., Ilikainen, M., 2019. Development of one-part alkali-activated ceramic/slag binders containing recycled ceramic aggregates. *J. Mater. Civ. Eng.* 31 (2).

Adesanya, E., Ohenoja, K., Luukkonen, T., Kinnunen, P., Ilikainen, M., 2018. One-part geopolymer cement from slag and pretreated paper sludge. *J. Cleaner Prod.* 185, 168–175.

Ahmari, S., Ren, X., Toufigh, V., Zhang, L., 2012. Production of geopolymeric binder from blended waste concrete powder and fly ash. *Constr. Build. Mater.* 35, 718–729.

Ajayi, S.O., Oyedele, L.O., Bilal, M., Akinade, O.O., Alaka, H.A., Owolabi, H.A., Kadiri, K.O., 2015. Waste effectiveness of the construction industry: understanding the impediments and requisites for improvements. *Resour. Conserv. Recycl.* 102, 101–112.

Akcaözöglü, S., Ulu, C., 2014. Recycling of waste PET granules as aggregate in alkali-activated blast furnace slag/metakaolin blends. *Constr. Build. Mater.* 58, 31–37.

Aly, S.T., Kanaan, D.M., El-Dieb, A.S., Abu-Eishah, S.I., 2018. Properties of ceramic waste powder-based geopolymer concrete. In: *International Congress on Polymers in Concrete*. Springer, pp. 429–435.

Aly, A.M., El-Feky, M.S., Kohail, M., Nasr, E.-S.A.R., 2019. Performance of geopolymer concrete containing recycled rubber. *Constr. Build. Mater.* 207, 136–144.

Amin, S.K., El-Sherbiny, S.A., El-Magd, A.A.M.A., Belal, A., Abadir, M.F., 2017. Fabrication of geopolymer bricks using ceramic dust waste. *Constr. Build. Mater.* 157, 610–620.

Antunes Boca Santa, R.A., Bernardin, A.M., Riella, H.G., Kuhnen, N.C., 2013. Geopolymer synthesized from bottom coal ash and calcined paper sludge. *J. Cleaner Prod.* 57, 302–307.

Arulrajah, A., Kua, T.-A., Horpibulsuk, S., Mirzababaei, M., Chinkulkijniwat, A., 2017. Recycled glass as a supplementary filler material in spent coffee grounds geopolymer. *Constr. Build. Mater.* 151, 18–27.

Ashraf, M.S., Ghouleh, Z., Shao, Y., 2019. Production of eco-cement exclusively from municipal solid waste incineration residues. *Resour. Conserv. Recycl.* 149, 332–342.

Avimieni, D., Peddinti, P.R.T., Saride, S., 2016. Durability and long term performance of geopolymer stabilized reclaimed asphalt pavement base courses. *Constr. Build. Mater.* 121, 198–209.

Azmi, A.A., Abdullah, M.M.A.B., Ghazali, C.M.R., Sandu, A.V., Hussin, K., 2016. Effect of crumb rubber on compressive strength of fly ash based geopolymer concrete. *MATEC Web of Conferences*. EDP Sciences p. 01063.

Azmi, A.A., Abdullah, M.M.A.B., Ghazali, C.M.R., Ahmad, R., Musa, L., Rou, L.S., 2019. The effect of different crumb rubber loading on the properties of fly ash-based geopolymer concrete. In: *IOP Conf. Ser.: Mater. Sci. Eng.* IOP Publishing. p. 012079.

Bernal, S., Ball, R., Hussein, O., Heath, A., Provis, J.L., 2014. Paper sludge ash as a precursor for production of alkali-activated materials. *Proceedings of the Second International Conference on Advances in Chemically-Activated Materials (CAM 2014)*.

Bhogayata, A.C., Arora, N.K., 2019. Utilization of metalized plastic waste of food packaging articles in geopolymer concrete. *J. Mater. Cycles Waste Manage.* 21 (4), 1014–1026.

Burciaga-Díaz, O., Durón-Sifuentes, M., Díaz-Guillén, J.A., Escalante-García, J.I., 2020. Effect of waste glass incorporation on the properties of geopolymers formulated with low purity metakaolin. *Cem. Concr. Compos.* 107.

Chen, Z., Liu, Y., Zhu, W., Yang, E.-H., 2016. Incinerator bottom ash (IBA) aerated geopolymer. *Constr. Build. Mater.* 112, 1025–1031.

Chen, Y., Cui, Z., Cui, X., Liu, W., Wang, X., Li, X., Li, S., 2019. Life cycle assessment of end-of-life treatments of waste plastics in China. *Resour. Conserv. Recycl.* 146, 348–357.

Dave, S., Bhogayata, A., Arora, N., 2017. Impact resistance of geopolymer concrete containing recycled plastic aggregates. *Kalpa Publications in Civil Engineering* 1, 137–143.

De Carvalho Gomes, S., Zhou, J.L., Li, W., Long, G., 2019. Progress in manufacture and properties of construction materials incorporating water treatment sludge: a review. *Resour. Conserv. Recycl.* 145, 148–159.

De Rossi, A., Ribeiro, M.J., Labrincha, J.A., Novais, R.M., Hotza, D., Moreira, R.F.P.M., 2019. Effect of the particle size range of construction and demolition waste on the fresh and hardened-state properties of fly ash-based geopolymer mortars with total replacement of sand. *Process Saf. Environ. Prot.* 129, 130–137.

Diaz-Loya, E.I., Allouche, E.N., Eklund, S., Joshi, A.R., Kupwade-Patil, K., 2012. Toxicity mitigation and solidification of municipal solid waste incinerator fly ash using alkaline activated coal ash. *Waste Manage.* 32 (8), 1521–1527.

Fořt, J., Vejmelková, E., Koňáková, D., Albová, N., Čáchová, M., Keppert, M., Rovnaníková, P., Černý, R., 2018. Application of waste brick powder in alkali activated aluminosilicates: functional and environmental aspects. *J. Cleaner Prod.* 194, 714–725.

Gandoman, M., Kokabi, M., 2015. Sound barrier properties of sustainable waste rubber/geopolymer concretes. *Iran. Polym. J.* 24 (2), 105–112.

Gao, X., Yuan, B., Yu, Q.L., Brouwers, H.J.H., 2017. Characterization and application of municipal solid waste incineration (MSWI) bottom ash and waste granite powder in alkali activated slag. *J. Cleaner Prod.* 164, 410–419.

Gluth, G.J.G., Lehmann, C., Rübner, K., Kühne, H.-C., 2014. Reaction products and strength development of wastepaper sludge ash and the influence of alkalis. *Cem. Concr. Compos.* 45, 82–88.

Gong, Y.F., Fang, Y.H., Yan, Y.R., Chen, L.Q., 2014. Investigation on alkali activated recycled cement mortar powder cementitious material. *Mater. Res. Innovations* 18 (suppl. 2) S2-784-S782-787.

Gualtieri, A.F., Veratti, L., Tucci, A., Esposito, L., 2012. Recycling of the product of thermal inertization of cement-asbestos in geopolymers. *Constr. Build. Mater.* 31, 47–51.

Gundupalli, S.P., Hait, S., Thakur, A., 2017. A review on automated sorting of source-separated municipal solid waste for recycling. *Waste Manage.* 60, 56–74.

Habert, G., d'Espinose de Lacaillerie, J.B., Roussel, N., 2011. An environmental evaluation of geopolymer based concrete production: reviewing current research trends. *J. Cleaner Prod.* 19 (11), 1229–1238.

Hajimohammadi, A., Ngo, T., Kashani, A., 2018. Glass waste versus sand as aggregates: the characteristics of the evolving geopolymer binders. *J. Cleaner Prod.* 193, 593–603.

Hassan, A., Arif, M., Shariq, M., 2019. Use of geopolymer concrete for a cleaner and sustainable environment – a review of mechanical properties and microstructure. *J. Cleaner Prod.* 223, 704–728.

Hoorweg, D., Bhada-Tata, P., 2012. *What a Waste: a Global Review of Solid Waste Management*. World Bank, Washington, DC.

- Hoy, M., Horpibulsuk, S., Arulrajah, A., 2016a. Strength development of Recycled Asphalt Pavement – fly ash geopolymer as a road construction material. *Constr. Build. Mater.* 117, 209–219.
- Hoy, M., Horpibulsuk, S., Rachan, R., Chinkulkijniwat, A., Arulrajah, A., 2016b. Recycled asphalt pavement - fly ash geopolymers as a sustainable pavement base material: strength and toxic leaching investigations. *Sci. Total Environ.* 573, 19–26.
- Hoy, M., Rachan, R., Horpibulsuk, S., Arulrajah, A., Mirzababaei, M., 2017. Effect of wetting-drying cycles on compressive strength and microstructure of recycled asphalt pavement – fly ash geopolymer. *Constr. Build. Mater.* 144, 624–634.
- Hoy, M., Horpibulsuk, S., Arulrajah, A., Mohajerani, A., 2018. Strength and micro-structural study of recycled asphalt pavement: slag geopolymer as a pavement base material. *J. Mater. Civ. Eng.* 30 (8).
- Hu, Y., Tang, Z., Li, W., Li, Y., Tam, V.W.Y., 2019. Physical-mechanical properties of fly ash/GBFS geopolymer composites with recycled aggregates. *Constr. Build. Mater.* 226, 139–151.
- Huang, Y., Bird, R.N., Heidrich, O., 2007. A review of the use of recycled solid waste materials in asphalt pavements. *Resour. Conserv. Recycl.* 52 (1), 58–73.
- Huang, B., Wang, X., Kua, H., Geng, Y., Bleischwitz, R., Ren, J., 2018a. Construction and demolition waste management in China through the 3R principle. *Resour. Conserv. Recycl.* 129, 36–44.
- Huang, G., Ji, Y., Li, J., Hou, Z., Jin, C., 2018b. Use of slaked lime and Portland cement to improve the resistance of MSWI bottom ash-GBFS geopolymer concrete against carbonation. *Constr. Build. Mater.* 166, 290–300.
- Huang, G., Ji, Y., Li, J., Zhang, L., Liu, X., Liu, B., 2019a. Effect of activated silica on polymerization mechanism and strength development of MSWI bottom ash alkali-activated mortars. *Constr. Build. Mater.* 201, 90–99.
- Huang, G., Ji, Y., Zhang, L., Hou, Z., Zhang, L., Wu, S., 2019b. Influence of calcium content on structure and strength of MSWI bottom ash-based geopolymer. *Mag. Concr. Res.* 71 (7), 362–372.
- Huseien, G.F., Ismail, M., Khalid, N.H.A., Hussin, M.W., Mirza, J., 2018a. Compressive strength and microstructure of assorted wastes incorporated geopolymer mortars: effect of solution molarity. *Alex. Eng. J.* 57 (4), 3375–3386.
- Huseien, G.F., Sam, A.R.M., Mirza, J., Tahir, M.M., Asaad, M.A., Ismail, M., Shah, K.W., 2018b. Waste ceramic powder incorporated alkali activated mortars exposed to elevated temperatures: performance evaluation. *Constr. Build. Mater.* 187, 307–317.
- Huseien, G.F., Sam, A.R.M., Shah, K.W., Asaad, M.A., Tahir, M.M., Mirza, J., 2019a. Properties of ceramic tile waste based alkali-activated mortars incorporating GBFS and fly ash. *Constr. Build. Mater.* 214, 355–368.
- Huseien, G.F., Sam, A.R.M., Shah, K.W., Mirza, J., Tahir, M.M., 2019b. Evaluation of alkali-activated mortars containing high volume waste ceramic powder and fly ash replacing GBFS. *Constr. Build. Mater.* 210, 78–92.
- Huseien, G.F., Sam, A.R.M., Shah, K.W., Mirza, J., 2020. Effects of ceramic tile powder waste on properties of self-compacted alkali-activated concrete. *Constr. Build. Mater.* 236.
- Hwang, C.-L., Damié Yehualaw, M., Vo, D.-H., Huynh, T.-P., 2019a. Development of high-strength alkali-activated pastes containing high volumes of waste brick and ceramic powders. *Constr. Build. Mater.* 218, 519–529.
- Hwang, C.-L., Yehualaw, M.D., Vo, D.-H., Huynh, T.-P., Largo, A., 2019b. Performance evaluation of alkali activated mortar containing high volume of waste brick powder blended with ground granulated blast furnace slag cured at ambient temperature. *Constr. Build. Mater.* 223, 657–667.
- Ji, Z., Pei, Y., 2019. Bibliographic and visualized analysis of geopolymer research and its application in heavy metal immobilization: a review. *J. Environ. Manage.* 231, 256–267.
- Jin, M., Zheng, Z., Sun, Y., Chen, L., Jin, Z., 2016. Resistance of metakaolin-MSWI fly ash based geopolymer to acid and alkaline environments. *J. Non-Cryst. Solids* 450, 116–122.
- Kathirvel, P., Kaliyaperumal, S.R.M., 2016. Influence of recycled concrete aggregates on the flexural properties of reinforced alkali activated slag concrete. *Constr. Build. Mater.* 102, 51–58.
- Kathirvel, P., Kaliyaperumal, S.R.M., 2017. Influence of recycled concrete aggregates on the engineering and durability properties of alkali activated slag concrete. *Constr. Build. Mater.* 133, 65–72.
- Keppert, M., Vejmelková, E., Bezdička, P., Doleželová, M., Čáchová, M., Scheinherrová, L., Pokorný, J., Vyšvařil, M., Rovnaníková, P., Černý, R., 2018. Red-clay ceramic powders as geopolymer precursors: consideration of amorphous portion and CaO content. *Appl. Clay Sci.* 161, 82–89.
- Khandelwal, H., Dhar, H., Thalla, A.K., Kumar, S., 2019. Application of life cycle assessment in municipal solid waste management: a worldwide critical review. *J. Cleaner Prod.* 209, 630–654.
- Khedmati, M., Kim, Y.-R., Turner, J.A., 2018. Investigation of the interphase between recycled aggregates and cementitious binding materials using integrated micro-structural-nanomechanical-chemical characterization. *Compos. Part B Eng.* 158, 218–229.
- Kinuthia, J., 2018. Wastepaper sludge ash. In: Siddique, R., Cachim, P. (Eds.), *Waste and Supplementary Cementitious Materials in Concrete*. Woodhead Publishing, pp. 289–321.
- Komnitsas, K., Zaharaki, D., Vlachou, A., Bartzas, G., Galetakis, M., 2015. Effect of synthesis parameters on the quality of construction and demolition wastes (CDW) geopolymers. *Adv. Powder Technol.* 26 (2), 368–376.
- Koushkbaghi, M., Alipour, P., Tahmouresi, B., Mohseni, E., Saradar, A., Sarker, P.K., 2019. Influence of different monomer ratios and recycled concrete aggregate on mechanical properties and durability of geopolymer concretes. *Constr. Build. Mater.* 205, 519–528.
- Kua, T.-A., Arulrajah, A., Mohammadinia, A., Horpibulsuk, S., Mirzababaei, M., 2017. Stiffness and deformation properties of spent coffee grounds based geopolymers. *Constr. Build. Mater.* 138, 79–87.
- Kua, T.-A., Imteaz, M.A., Arulrajah, A., Horpibulsuk, S., 2018. Environmental and economic viability of Alkali activated Material (AAM) comprising slag, fly ash and spent coffee ground. *Int. J. Sustainable Eng.* 12 (4), 223–232.
- Kurda, R., Silvestre, J.D., de Brito, J., 2018. Life cycle assessment of concrete made with high volume of recycled concrete aggregates and fly ash. *Resour. Conserv. Recycl.* 139, 407–417.
- Łach, M., Kiszka, A., Korniejenko, K., Mikula, J., 2018. The mechanical properties of waste tire cords reinforced geopolymer concretes. In: *IOP Conf. Ser.: Mater. Sci. Eng.* IOP Publishing, p. 012089.
- Lancellotti, I., Kamsu, E., Michelazzi, M., Barbieri, L., Corradi, A., Leonelli, C., 2010. Chemical stability of geopolymers containing municipal solid waste incinerator fly ash. *Waste Manage.* 30 (4), 673–679.
- Lancellotti, I., Ponzoni, C., Barbieri, L., Leonelli, C., 2013. Alkali activation processes for incinerator residues management. *Waste Manage.* 33 (8), 1740–1749.
- Lancellotti, I., Cannio, M., Bollino, F., Catauro, M., Barbieri, L., Leonelli, C., 2015. Geopolymers: an option for the valorization of incinerator bottom ash derived “end of waste”. *Ceram. Int.* 41 (2), 2116–2123.
- Laurent, A., Bakas, I., Clavreul, J., Bernstad, A., Niero, M., Gentil, E., Hauschild, M.Z., Christensen, T.H., 2014. Review of LCA studies of solid waste management systems—part I: lessons learned and perspectives. *Waste Manage.* 34 (3), 573–588.
- Lee, N.K., Abate, S.Y., Kim, H.-K., 2018. Use of recycled aggregates as internal curing agent for alkali-activated slag system. *Constr. Build. Mater.* 159, 286–296.
- Li, Y., Min, X., Ke, Y., Liu, D., Tang, C., 2019. Preparation of red mud-based geopolymer materials from MSWI fly ash and red mud by mechanical activation. *Waste Manage.* 83, 202–208.
- Liu, Z., Cai, C.S., Peng, H., Fan, F., 2016. Experimental study of the geopolymeric recycled aggregate concrete. *J. Mater. Civ. Eng.* 28 (9).
- Liu, C., Deng, X., Liu, J., Hui, D., 2019a. Mechanical properties and microstructures of hypergolic and calcined coal gangue based geopolymer recycled concrete. *Constr. Build. Mater.* 221, 691–708.
- Liu, D.G., Ke, Y., Min, X.B., Liang, Y.J., Wang, Z.B., Li, Y.C., Fei, J.C., Yao, L.W., Xu, H., Jiang, G.H., 2019b. Cotreatment of MSWI fly ash and granulated lead smelting slag using a geopolymer system. *Int. J. Environ. Res. Public Health* 16 (1).
- Liu, Y., Shi, C., Zhang, Z., Li, N., 2019c. An overview on the reuse of waste glasses in alkali-activated materials. *Resour. Conserv. Recycl.* 144, 297–309.
- Long, W.-J., Li, H.-D., Wei, J.-J., Xing, F., Han, N., 2018. Sustainable use of recycled crumb rubbers in eco-friendly alkali activated slag mortar: dynamic mechanical properties. *J. Cleaner Prod.* 204, 1004–1015.
- Lu, J.-X., Poon, C.S., 2018. Use of waste glass in alkali activated cement mortar. *Constr. Build. Mater.* 160, 399–407.
- Luhar, S., Chaudhary, S., Luhar, I., 2018. Thermal resistance of fly ash based rubberized geopolymer concrete. *J. Build. Eng.* 19, 420–428.
- Luhar, S., Chaudhary, S., Luhar, I., 2019a. Development of rubberized geopolymer concrete: strength and durability studies. *Constr. Build. Mater.* 204, 740–753.
- Luhar, S., Cheng, T.-W., Luhar, I., 2019b. Incorporation of natural waste from agricultural and aquacultural farming as supplementary materials with green concrete: a review. *Compos. Part B Eng.* 175.
- Luhar, S., Cheng, T.-W., Nicolaides, D., Luhar, I., Panias, D., Sakkas, K., 2019c. Valorisation of glass waste for development of Geopolymer composites – mechanical properties and rheological characteristics: a review. *Constr. Build. Mater.* 220, 547–564.
- Luhar, S., Cheng, T.-W., Nicolaides, D., Luhar, I., Panias, D., Sakkas, K., 2019d. Valorisation of glass waste for the development of geopolymer composites – durability, thermal and microstructural properties: a review. *Constr. Build. Mater.* 222, 673–687.
- Luna Galiano, Y., Fernandez Pereira, C., Vale, J., 2011. Stabilization/solidification of a municipal solid waste incineration residue using fly ash-based geopolymers. *J. Hazard. Mater.* 185 (1), 373–381.
- Mamat, N., Kusbantoro, A., Rahman, N., 2018. Hydrochloric acid based pre-treatment on paper mill sludge ash as an alternative source material for geopolymer. *Mater. Today: Proc.* 5 (10), 21825–21831.
- Menegaki, M., Damigos, D., 2018. A review on current situation and challenges of construction and demolition waste management. *Curr. Opin. Green Sustainable Chem.* 13, 8–15.
- Meng, Y., Ling, T.-C., Mo, K.H., 2018. Recycling of wastes for value-added applications in concrete blocks: an overview. *Resour. Conserv. Recycl.* 138, 298–312.
- Moghadam, M.J., Ajalloeian, R., Hajiannia, A., 2019. Preparation and application of alkali-activated materials based on waste glass and coal gangue: a review. *Constr. Build. Mater.* 221, 84–98.
- Mohammadinia, A., Arulrajah, A., Sanjayan, J., Disfani, M.M., Bo, M.W., Darmawan, S., 2016a. Stabilization of demolition materials for pavement base/subbase applications using fly ash and slag geopolymers: laboratory investigation. *J. Mater. Civ. Eng.* 28 (7).
- Mohammadinia, A., Arulrajah, A., Sanjayan, J., Disfani, M.M., Bo, M.W., Darmawan, S., 2016b. Strength development and microfabric structure of construction and demolition aggregates stabilized with fly ash-based geopolymers. *J. Mater. Civ. Eng.* 28 (11).
- Mohammed, B.S., Liew, M.S., Alaloul, W., Al-Fakh, A., Ibrahim, W., Adamu, M., 2018. Development of rubberized geopolymer interlocking bricks. *Case Stud. Constr. Mater.* 8, 401–408.
- Navarro, R., Alcocel, E.G., Sánchez, I., Garcés, P., Zornoza, E., 2018. Mechanical properties of alkali activated ground SiMn slag mortars with different types of aggregates. *Constr. Build. Mater.* 186, 79–89.
- Novais, R.M., Saeli, M., Caetano, A.P.F., Seabra, M.P., Labrincha, J.A., Surendran, K.P., Pullar, R.C., 2019. Pyrolysed cork-geopolymer composites: a novel and sustainable

- EMI shielding building material. *Constr. Build. Mater.* 229.
- Nuaklong, P., Sata, V., Chindaprasirt, P., 2016. Influence of recycled aggregate on fly ash geopolymer concrete properties. *J. Cleaner Prod.* 112, 2300–2307.
- Nuaklong, P., Sata, V., Chindaprasirt, P., 2018a. Properties of metakaolin-high calcium fly ash geopolymer concrete containing recycled aggregate from crushed concrete specimens. *Constr. Build. Mater.* 161, 365–373.
- Nuaklong, P., Sata, V., Wongsas, A., Srinavin, K., Chindaprasirt, P., 2018b. Recycled aggregate high calcium fly ash geopolymer concrete with inclusion of OPC and nano-SiO₂. *Constr. Build. Mater.* 174, 244–252.
- Onuaguluchi, O., Borges, P.H.R., Bhutta, A., Banthia, N., 2017. Performance of scrap tire steel fibers in OPC and alkali-activated mortars. *Mater. Struct.* 50 (2).
- Ouda, A.S., 2019. Development the properties of brick geopolymer pastes using concrete waste incorporating dolomite aggregate. *J. Build. Eng.* 27, 100919.
- Park, Y., Abolmaali, A., Kim, Y.H., Ghahremannejad, M., 2016. Compressive strength of fly ash-based geopolymer concrete with crumb rubber partially replacing sand. *Constr. Build. Mater.* 118, 43–51.
- Part, W.K., Ramli, M., Cheah, C.B., 2015. An overview on the influence of various factors on the properties of geopolymer concrete derived from industrial by-products. *Constr. Build. Mater.* 77, 370–395.
- Patel, R., Bhogayata, A., Arora, N., Parmar, K., 2013. Flexural response of geopolymer concrete beam containing metallized plastic waste. *Int. J. Adv. Eeg. Technol.* 72, 72–74.
- Payne, J., Joussein, E., Gautron, J., Doudeau, J., Rossignol, S., 2017. Feasibility of producing geopolymer binder based on a brick clay mixture. *Ceram. Int.* 43 (13), 9860–9871.
- Posi, P., Ridditrud, C., Ekvong, C., Chammanee, D., Janthowong, K., Chindaprasirt, P., 2015. Properties of lightweight high calcium fly ash geopolymer concretes containing recycled packaging foam. *Constr. Build. Mater.* 94, 408–413.
- Posi, P., Thongjapo, P., Thamultree, N., Boontee, P., Kasemsiri, P., Chindaprasirt, P., 2016. Pressed lightweight fly ash-OPC geopolymer concrete containing recycled lightweight concrete aggregate. *Constr. Build. Mater.* 127, 450–456.
- Provis, J.L., 2013. Geopolymers and other alkali activated materials: why, how, and what? *Mater. Struct.* 47 (1–2), 11–25.
- Provis, J.L., Palomo, A., Shi, C., 2015. Advances in understanding alkali-activated materials. *Cem. Concr. Res.* 78, 110–125.
- Rakhimova, N.R., Rakhimov, R.Z., 2015. Alkali-activated cements and mortars based on blast furnace slag and red clay brick waste. *Mater. Des.* 85, 324–331.
- Ramos, G.A., Pelisser, F., Paul Gleize, P.J., Bernardin, A.M., Michel, M.D., 2018. Effect of porcelain tile polishing residue on geopolymer cement. *J. Cleaner Prod.* 191, 297–303.
- Reddy, M.S., Dinakar, P., Rao, B.H., 2016. A review of the influence of source material's oxide composition on the compressive strength of geopolymer concrete. *Microporous Mesoporous Mater.* 234, 12–23.
- Reig, L., Tashima, M.M., Borrachero, M.V., Monzó, J., Cheeseman, C.R., Payá, J., 2013a. Properties and microstructure of alkali-activated red clay brick waste. *Constr. Build. Mater.* 43, 98–106.
- Reig, L., Tashima, M.M., Soriano, L., Borrachero, M.V., Monzó, J., Payá, J., 2013b. Alkaline activation of ceramic waste materials. *Waste Biomass Valorization* 4 (4), 729–736.
- Reig, L., Soriano, L., Borrachero, M.V., Monzó, J., Payá, J., 2016. Influence of calcium aluminate cement (CAC) on alkaline activation of red clay brick waste (RCBW). *Cem. Concr. Compos.* 65, 177–185.
- Reig, L., Sanz, M.A., Borrachero, M.V., Monzó, J., Soriano, L., Payá, J., 2017. Compressive strength and microstructure of alkali-activated mortars with high ceramic waste content. *Ceram. Int.* 43 (16), 13622–13634.
- Ridzuan, A., Khairulniza, A., Fadzil, M., Nurliza, J., Fauzi, M., Yusoff, W., 2014a. Alkaline activators concentration effect to strength of waste paper sludge ash-based geopolymer mortar. In: *Proceedings of the International Civil and Infrastructure Engineering Conference 2013*. Springer. pp. 169–175.
- Ridzuan, A.R.M., Khairulniza, A.A., Fadzil, M.A., Nurliza, J., 2014b. Effect of alkaline activators concentration to the strength and morphological properties of wastepaper-based geopolymer mortars. *Mater. Sci. Forum* 803, 88–92.
- Robayo, R.A., Mulford, A., Munera, J., Mejía de Gutiérrez, R., 2016. Alternative cements based on alkali-activated red clay brick waste. *Constr. Build. Mater.* 128, 163–169.
- Rovnanik, P., Rovnaniková, P., Vyšvařil, M., Grzeszczyk, S., Janowska-Renkas, E., 2018. Rheological properties and microstructure of binary waste red brick powder/metakaolin geopolymer. *Constr. Build. Mater.* 188, 924–933.
- Saikia, N., de Brito, J., 2012. Use of plastic waste as aggregate in cement mortar and concrete preparation: a review. *Constr. Build. Mater.* 34, 385–401.
- Sanusi, O., Tempest, B., Ogunro, V., Gergely, J., 2016. Leaching characteristics of geopolymer cement concrete containing recycled concrete aggregates. *J. Hazard. Toxic Radioact. Waste* 20 (3), 04016002.
- Saride, S., Avirneni, D., Challapalli, S., 2016. Micro-mechanical interaction of activated fly ash mortar and reclaimed asphalt pavement materials. *Constr. Build. Mater.* 123, 424–435.
- Sarmiento, L.M., Clavier, K.A., Paris, J.M., Ferraro, C.C., Townsend, T.G., 2019. Critical examination of recycled municipal solid waste incineration ash as a mineral source for Portland cement manufacture – a case study. *Resour. Conserv. Recycl.* 148, 1–10.
- Sata, V., Wongsas, A., Chindaprasirt, P., 2013. Properties of pervious geopolymer concrete using recycled aggregates. *Constr. Build. Mater.* 42, 33–39.
- Sedaghatdoost, A., Behfarnia, K., Bayati, M., Vaezi, Ms., 2019. Influence of recycled concrete aggregates on alkali-activated slag mortar exposed to elevated temperatures. *J. Build. Eng.* 26.
- Sedira, N., Castro-Gomes, J., Magrinho, M., 2018. Red clay brick and tungsten mining waste-based alkali-activated binder: microstructural and mechanical properties. *Constr. Build. Mater.* 190, 1034–1048.
- Shaikh, F.U.A., 2016. Mechanical and durability properties of fly ash geopolymer concrete containing recycled coarse aggregates. *Int. J. Sustainable Built Environ.* 5 (2), 277–287.
- Shi, X.S., Collins, F.G., Zhao, X.L., Wang, Q.Y., 2012. Mechanical properties and microstructure analysis of fly ash geopolymer recycled concrete. *J. Hazard. Mater.* 237–238, 20–29.
- Shi, C., Li, Y., Zhang, J., Li, W., Chong, L., Xie, Z., 2016. Performance enhancement of recycled concrete aggregate – a review. *J. Cleaner Prod.* 112, 466–472.
- Shiota, K., Nakamura, T., Takaoka, M., Nitta, K., Oshita, K., Fujimori, T., Ina, T., 2017. Chemical kinetics of Cs species in an alkali-activated municipal solid waste incineration fly ash and pyrophyllite-based system using Cs K-edge in situ X-ray absorption fine structure analysis. *Spectrochim. Acta, Part B* 131, 32–39.
- Shoaei, P., Musaei, H.R., Mirlohi, F., Narimani zamanabadi, S., Ameri, F., Bahrami, N., 2019. Waste ceramic powder-based geopolymer mortars: effect of curing temperature and alkaline solution-to-binder ratio. *Constr. Build. Mater.* 227, 116686.
- Si, R., Dai, Q., Guo, S., Wang, J., 2020. Mechanical property, nanopore structure and drying shrinkage of metakaolin-based geopolymer with waste glass powder. *J. Cleaner Prod.* 242, 118502.
- Siddique, R., 2010a. Use of municipal solid waste ash in concrete. *Resour. Conserv. Recycl.* 55 (2), 83–91.
- Siddique, R., 2010b. Utilization of municipal solid waste (MSW) ash in cement and mortar. *Resour. Conserv. Recycl.* 54 (12), 1037–1047.
- Silva, G., Castañeda, D., Kim, S., Castañeda, A., Bertolotti, B., Ortega-San-Martin, L., Nakamatsu, J., Aguilar, R., 2019a. Analysis of the production conditions of geopolymer matrices from natural pozzolana and fired clay brick wastes. *Constr. Build. Mater.* 215, 633–643.
- Silva, R.V., de Brito, J., Lynn, C.J., Dhir, R.K., 2019b. Environmental impacts of the use of bottom ashes from municipal solid waste incineration: a review. *Resour. Conserv. Recycl.* 140, 23–35.
- Spasiano, D., Pirozzi, F., 2017. Treatments of asbestos containing wastes. *J. Environ. Manage.* 204 (Pt 1), 82–91.
- Suksiripattanapong, C., Kua, T.-A., Arulrajah, A., Maghool, F., Horpibulsuk, S., 2017. Strength and microstructure properties of spent coffee grounds stabilized with rice husk ash and slag geopolymers. *Constr. Build. Mater.* 146, 312–320.
- Sun, Z., Cui, H., An, H., Tao, D., Xu, Y., Zhai, J., Li, Q., 2013. Synthesis and thermal behavior of geopolymer-type material from waste ceramic. *Constr. Build. Mater.* 49, 281–287.
- Sun, L., Fujii, M., Tasaki, T., Dong, H., Ohnishi, S., 2018. Improving waste to energy rate by promoting an integrated municipal solid-waste management system. *Resour. Conserv. Recycl.* 136, 289–296.
- Tang, Z., Hu, Y., Li, W., Tam, V.W.Y., 2019a. Uniaxial compressive behaviors of fly ash/slag-based geopolymer concrete with recycled aggregates. *Cem. Concr. Compos.* 104, 103375.
- Tang, Z., Li, W., Hu, Y., Zhou, J.L., Tam, V.W.Y., 2019b. Review on designs and properties of multifunctional alkali-activated materials (AAMs). *Constr. Build. Mater.* 200, 474–489.
- Tang, Z., Li, W., Tam, V.W.Y., Luo, Z., 2020. Investigation on dynamic mechanical properties of fly ash/slag-based geopolymer recycled aggregate concrete. *Compos. Part B Eng.* 185, 107776.
- Thomas, B.S., Gupta, R.C., 2016. A comprehensive review on the applications of waste tire rubber in cement concrete. *Renewable Sustainable Energy Rev.* 54, 1323–1333.
- Tome, S., Etoh, M.-A., Etame, J., Sanjay, K., 2018. Characterization and leachability behaviour of geopolymer cement synthesised from municipal solid waste incinerator fly ash and volcanic ash blends. *Recycl.* 3 (4).
- Tuyan, M., Andiç-Çakır, Ö., Ramyar, K., 2018. Effect of alkali activator concentration and curing condition on strength and microstructure of waste clay brick powder-based geopolymer. *Compos. Part B Eng.* 135, 242–252.
- Usha, S., Nair, D.G., Vishnudas, S., 2016. Feasibility study of geopolymer binder from terracotta roof tile waste. *Procedia Technol.* 25, 186–193.
- Vásquez, A., Cárdenas, V., Robayo, R.A., de Gutiérrez, R.M., 2016. Geopolymer based on concrete demolition waste. *Adv. Powder Technol.* 27 (4), 1173–1179.
- Verian, K.P., Ashraf, W., Cao, Y., 2018. Properties of recycled concrete aggregate and their influence in new concrete production. *Resour. Conserv. Recycl.* 133, 30–49.
- Vinai, R., Soutsos, M., 2019. Production of sodium silicate powder from waste glass cullet for alkali activation of alternative binders. *Cem. Concr. Res.* 116, 45–56.
- Waste Atlas, 2019. D-Waste. (accessed 10.21.2019). <http://www.atlas.d-waste.com/>.
- Wongkavanklom, A., Posi, P., Homwuttivong, S., Sata, V., Wongsas, A., Tanangteerapong, D., Chindaprasirt, P., 2019. Lightweight geopolymer concrete containing recycled plastic beads. *Key Eng. Mater.* 801, 377–384.
- Wongsas, A., Sata, V., Nematollahi, B., Sanjayan, J., Chindaprasirt, P., 2018a. Mechanical and thermal properties of lightweight geopolymer mortar incorporating crumb rubber. *J. Cleaner Prod.* 195, 1069–1080.
- Wongsas, A., Sata, V., Nuaklong, P., Chindaprasirt, P., 2018b. Use of crushed clay brick and pumice aggregates in lightweight geopolymer concrete. *Constr. Build. Mater.* 188, 1025–1034.
- Xie, J., Wang, J., Rao, R., Wang, C., Fang, C., 2018. Effects of combined usage of GGBS and fly ash on workability and mechanical properties of alkali activated geopolymer concrete with recycled aggregate. *Compos. Part B Eng.* 164, 179–190.
- Xie, J., Chen, W., Wang, J., Fang, C., Zhang, B., Liu, F., 2019a. Coupling effects of recycled aggregate and GGBS/metakaolin on physicochemical properties of geopolymer concrete. *Constr. Build. Mater.* 226, 345–359.
- Xie, J., Wang, J., Zhang, B., Fang, C., Li, L., 2019b. Physicochemical properties of alkali activated GGBS and fly ash geopolymer recycled concrete. *Constr. Build. Mater.* 204, 384–398.
- Xu, J.-J., Chen, Z.-P., Xiao, Y., Demartino, C., Wang, J.-H., 2017. Recycled aggregate concrete in FRP-confined columns: a review of experimental results. *Compos. Struct.*

- 174, 277–291.
- Xu, J.-J., Chen, Z.-P., Ozbakkaloglu, T., Zhao, X.-Y., Demartino, C., 2018. A critical assessment of the compressive behavior of reinforced recycled aggregate concrete columns. *Eng. Struct.* 161, 161–175.
- Xu, P., Zhao, Q., Qiu, W., Xue, Y., Li, N., 2019. Microstructure and strength of alkali-activated bricks containing municipal solid waste Incineration (MSWI) fly ash developed as construction materials. *Sustainability* 11 (5).
- Xuan, D., Poon, C.S., Zheng, W., 2018. Management and sustainable utilization of processing wastes from ready-mixed concrete plants in construction: a review. *Resour. Conserv. Recycl.* 136, 238–247.
- Xuan, D., Tang, P., Poon, C.S., 2019. MSWIBA-based cellular alkali-activated concrete incorporating waste glass powder. *Cem. Concr. Compos.* 95, 128–136.
- Yahya, Z., Abdullah, M., Ramli, S., Minciuna, M., Razak, R.A., 2018. Durability of fly ash based geopolymer concrete infilled with rubber crumb in seawater exposure. In: *IOP Conf. Ser.: Mater. Sci. Eng.* IOP Publishing. p. 012069.
- Yan, S., Sagoe-Crentsil, K., 2012. Properties of wastepaper sludge in geopolymer mortars for masonry applications. *J. Environ. Manage.* 112, 27–32.
- Yan, S., Sagoe-Crentsil, K., 2016. Evaluation of fly ash geopolymer mortar incorporating calcined wastepaper sludge. *J. Sustain. Cem. Mater.* 5 (6), 370–380.
- Ye, N., Chen, Y., Yang, J., Liang, S., Hu, Y., Xiao, B., Huang, Q., Shi, Y., Hu, J., Wu, X., 2016. Co-disposal of MSWI fly ash and Bayer red mud using an one-part geopolymeric system. *J. Hazard. Mater.* 318, 70–78.
- Yliniemi, J., Luukkonen, T., Kaiser, A., Illikainen, M., 2019. Mineral wool waste-based geopolymers. In: *IOP Conf. Ser.: Earth Environ. Sci.* IOP Publishing. p. 012006.
- Zaumanis, M., Mallick, R.B., Frank, R., 2014. 100% recycled hot mix asphalt: a review and analysis. *Resour. Conserv. Recycl.* 92, 230–245.
- Zawrah, M.F., Gado, R.A., Feltin, N., Ducourtieux, S., Devoille, L., 2016. Recycling and utilization assessment of waste fired clay bricks (Grog) with granulated blast-furnace slag for geopolymer production. *Process Saf. Environ. Prot.* 103, 237–251.
- Zhao, S., Muhammad, F., Yu, L., Xia, M., Huang, X., Jiao, B., Lu, N., Li, D., 2019. Solidification/stabilization of municipal solid waste incineration fly ash using uncalcined coal gangue-based alkali-activated cementitious materials. *Environ. Sci. Pollut. Res.* 26 (25), 25609–25620.
- Zheng, L., Wang, C., Wang, W., Shi, Y., Gao, X., 2011. Immobilization of MSWI fly ash through geopolymerization: effects of water-wash. *Waste Manage.* 31 (2), 311–317.
- Zheng, L., Wang, W., Gao, X., 2016. Solidification and immobilization of MSWI fly ash through aluminate geopolymerization: based on partial charge model analysis. *Waste Manage.* 58, 270–279.
- Zhong, H., Poon, E.W., Chen, K., Zhang, M., 2019. Engineering properties of crumb rubber alkali-activated mortar reinforced with recycled steel fibres. *J. Cleaner Prod.*
- Zhu, W., Rao, X.H., Liu, Y., Yang, E.-H., 2018. Lightweight aerated metakaolin-based geopolymer incorporating municipal solid waste incineration bottom ash as gas-forming agent. *J. Cleaner Prod.* 177, 775–781.
- Zhu, W., Chen, X., Struble, L.J., Yang, E.-H., 2019a. Quantitative characterization of aluminosilicate gels in alkali-activated incineration bottom ash through sequential chemical extractions and deconvoluted nuclear magnetic resonance spectra. *Cem. Concr. Compos.* 99, 175–180.
- Zhu, W., Teoh, P.J., Liu, Y., Chen, Z., Yang, E.-H., 2019b. Strategic utilization of municipal solid waste incineration bottom ash for the synthesis of lightweight aerated alkali-activated materials. *J. Cleaner Prod.* 235, 603–612.